

2023

Corporate Guidance



**SPD Laboratory, Inc.
Hamamatsu 432-8011,
JAPAN**

"For Successful
Future R&D of
State-of-the-Art Thin
Film Formation and
Next Generation Solar
Cells"

Mission

We aim to introduce next-generation technology on the thin-film formation and solar cell fabrication towards scientists and engineers and then to make peoples' lives more comfortable by putting our accumulated intellectual properties to the solution of clean energy supply and environmental preservation problems in line with SDGs.



Shoji Kaneko, Ph.D.
Director

Corporate History

In 2004 Dr. S. Kaneko has founded the SPD Laboratory with the goal of spreading a spray pyrolysis deposition (SPD) for functional thin-film formation which he had been developing during his time at Shizuoka University since 1989. Bridging the gap between academia and industry with creative and tailor-made products has been our target from the beginning. Nowadays we are producing SPD machines, constructing dye-sensitized and perovskite solar cell fabrication systems, and developing further solar cell evaluation systems. Our company's target is to supply customers the products of the best quality at a reasonable price.

What is a Spray Pyrolysis Deposition?

(1) Principles

Our SPD for functional thin film formation is basically performed under atmospheric pressure using simple apparatus consisting of an atomizer, air compressor, solution reservoir, and heater (Fig. 1). Starting raw materials solution is atomized towards heated substrate by a pneumatic system not consecutively but intermittently to hold a constant substrate temperature because a mixture of solution and air atomized lets the substrate temperature reduce.

Inorganic and organic metal compounds having any adapted solvent are all available as raw materials of SPD process. The original component and composition of starting solution are surely reflected in the deposited film except for easily evaporated additives; accordingly, this method gives the prescribed component and composition of film as planned.

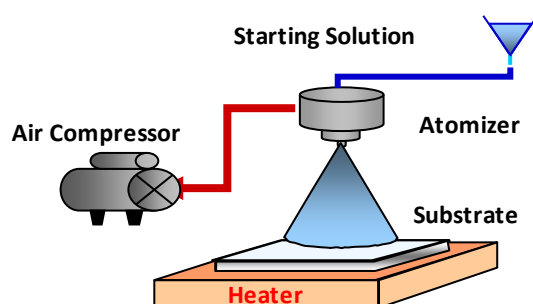


Fig. 1. Schematic diagram of SPD apparatus.

(2) Deposition Process

Solid film deposition from liquid phase occurs in succession according to the following steps shown in Fig. 2:

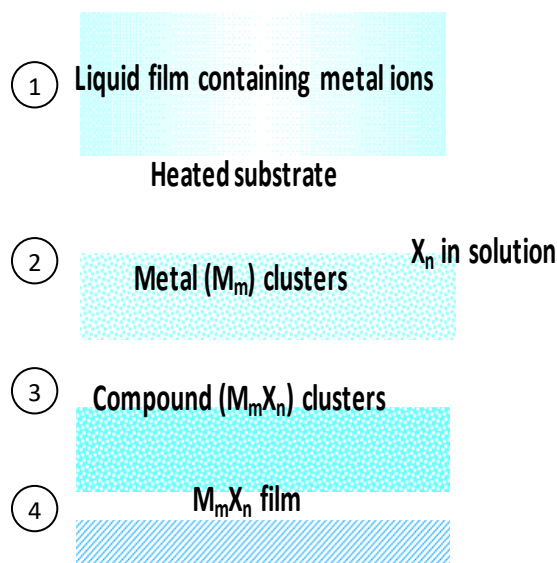


Fig. 2. Film deposition process.

- ① Innumerable mists from an atomizer wet to make liquid film on the substrate just after sprayed and the boiling temperature of a solvent can be kept until its complete evaporation according to the Gibbs' Phase Rule, despite the substrate temperature which is set much higher than the boiling temperature of the solvent.
- ② Temperature of the remained solute increases rapidly to yield metal clusters throughout thermal decomposition and/or chemical reaction.
- ③ Metal clusters could be converted instantly to compound clusters by reacting with negative ions in the solution.
- ④ Condensation and cohesion of these compound clusters on the substrate yield solid film finally.

(3) Features

SPD is one of the chemical thin film formation methods and makes dense and even thin films with film thickness 10 nm to 10 μm from starting solution. Complex compound and solid solution films are also available as non-equilibrium or meta-stable phases according to the control of starting solutions and substrate temperatures. The shape and size of particles in polycrystalline film, the microstructure, and texture are controllable by choosing deposition conditions. Further, film thickness increases in proportion to the concentration of starting solution, spray rate and time, and the number of cycles, and is affected by substrate temperature, the vapor pressure of solute, and wetting ability of starting solution.

It has been speculated that atomic diffusion or movement occurs to advance the crystallization of fine particles and the densification of texture in film, while the atomizing is stopped for avoiding the reduction of substrate temperature. This stopping could contribute to the quality of the deposited film.

Promising Future Developments

- **Manufacturing and Sales of Transparent Conductive Oxide Thin Film (TCO)**

We will use the SPD technique to prepare fluorine-doped tin oxide (FTO) and tin-doped indium oxide (ITO) thin films on a glass surface, which have high performance of electrical conductivity and visible light transmittance. These TCOs are applicable to display panels of cell phones, electromagnetic shielding glass, solar cells, and so on.

- **R&D on Dye-sensitized Solar Cell (DSC) and Perovskite Solar Cell (PSC)**

DSC consists of two kinds of an electrode; one is a photoelectrode coated with a porous layer of wide band-gap semiconductor and dye. The other is a counter electrode coated with a very thin layer of platinum. The space between these two electrodes is filled with an electrolyte.

Without any ultra-vacuum system, hazardous materials, and also with low cost, DSC and PSC both are attractive as next-generation solar cells in place of current expensive silicon solar cells. It is probable to save up to more than 50% of the cost by switching to DSC and PSC.

We have further initiated the research of PSC processing with a piezoelectric-inkjet-printing technology, and PV power analyzers with MPPT technique. global warming due to fossil fuel-based power plants and high risk with unmanageable radioactive waste in the nuclear power plants make those two energy production techniques not suitable for the future world.

We wish to contribute continuously to the development of next-generation solar cell research

making a connection with a better solution to these problems through collaboration with highly motivated scientists and engineers.

- **Supply of Novel Solar Cell Evaluation Systems**

We have developed the first generation PV Power Analyzer VK-PA-25 (discontinued) with built-in Maximum Power Point Tracking (MPPT) function in 2015 and then delivered it to Prof. Segawa Group at the RCAST, University of Tokyo. By utilizing this, Prof. S. Uchida has patiently continued his research on PSC hysteresis and used the discussion on MPPT technique to evaluate real solar cell performance. This announcement was new to everyone's memory. Particularly it was significant to clarify that the hysteresis of a stacked PSC was caused by its internal capacitance component. Built-in MPPT function in all of our PV Power Analyzers utilizes firmware level advanced MPPT algorithm which effectively maintains the cell at the maximum output conditions. This has been used in the evaluation of real solar cell performance which is different from the conventional I-V curve method.

Subsequently, other power analyzers, capacitance analyzers for thin film and supercapacitor, LED solar simulators have been developed so far.

- **Instrumentation for solar cell fabrication and power storage process.**

Clean and enormous energy supply is an urgent demand for favorable economic growth all over the world. We would like to construct photovoltaics with DSC/PSC and power storage with a battery/supercapacitor combined system for the achievement of this request just from now, making the use of our different experiences.

Thin Film Formation Systems



KV-100
(SPD)



KM-300
(SPD)



VK-TFP-120
(Ink-jet Printing & Dispensing)

PV Power Analyzers & Super Capacitor and Battery Analyzer



VK-PA-100



VK-PA-Pico



VK-CA-1000



VK-CA-8000

Papers

1. G.R.A. Kumara et al., "Large area dye-sensitized solar cells with titanium based counter electrode," *Thin Solid Films*, 520 (2012) 4119-21.
2. P.V.V. Jayaweera and S. Kaneko, "Fabrication of Automatic Electrolyte Filling Machine for Dye-sensitized Solar Cells," *Instr. Sci. Technol.*, 40 (2012) 490-503.
3. E.V.A. Premalal et al., "Development of Quality FTO Films by Spray Pyrolysis for Dye-sensitized Solar Cell," *Electrochemistry*, 80 (2012) 624-28.
4. E.V.A. Premalal et al., "Preparation of high quality spray-deposited fluorine-doped tin oxide thin films using dilute di(n-butyl)tin(IV) diacetate precursor solutions," *Thin Solid Films*, 520 (2012) 6813-17.
5. D. Liyanage et al., "Ethylene glycol assisted synthesis of fluorine doped tin oxide nanorods using improved spray pyrolysis deposition method," *Applied Physics Express*, 6 (2013) 085501.
6. Ludmila Cojocaru et al., "Origin of the Hysteresis in I-V Curves for Planar Structure Perovskite Solar Cells Rationalized with a Surface Boundary Induced Capacitance Model," *Chem. Lett.*, 44 (2015) 1750-52.
7. Yadav Pankaj et al., "Electroanalytical investigation of the losses during interfacial charge transport in dye-sensitized solar cell," *Solar Energy*, 129 (2016) 207-216.
8. Ludmila Cojocaru et al., "Simulation of current –voltage curves for inverted planer structure perovskite solar cells using equivalent circuit model with inductance," *Appl. Phys. Express*, 10 (2017) 025701.
9. Ludmila Cojocaru et al., Reply to "Comment on 'Simulation of current –voltage curves for inverted planer structure perovskite solar cells using equivalent circuit model with inductance'" *Appl. Phys. Express*, 10 (2017) 059102.
10. Ludmila Cojocaru et al., "Determination of unique power conversion efficiency of solar cell showing hysteresis in the I-V curve under various light intensities," *Scientific Reports*, 7 (2017) 11790.
11. Ludmila Cojocaru et al., "Effect of TiO₂ Surface Treatment on the Current-Voltage Hysteresis of Planer-Structure Perovskite Solar Cells Prepared on Rough and Flat Fluorine-Doped Tin Oxide Substrates," *Energy Technol.* 5 (2017) 1-5

Patents

- 1) JP4841574 "Dye-sensitized solar cell module and its fabrication method"
- 2) JP4945491 "Multilayered electrode and dye-sensitized solar cell with its electrode"
- 3) JP5227194 "Multilayered electrodes"
- 4) JP5743591 "Thin-film formation method and apparatus, and dye-sensitized solar cell fabrication process and its production system"
- 5) JP5963902 "Dye-sensitized solar cell fabrication process and its production system"
- 6) JP5979656 2 "Ultraviolet irradiation and curing apparatus"



KV-25II



Specifications

Substrate size	Up to 25 mm × 25 mm
Substrate temperature	Max. 550 °C
Spray distance	150 mm to 300 mm (with ±0.5 mm accuracy)
Reaction chamber	W320 mm x D360 x H360 mm Teflon coated for corrosion resistance
External dimensions	W650 mm x D500 mm x H820 mm
Weight	60 kg
Capacity of solution bottle	250 ml

Features

Rotating spray nozzle	Spray nozzle is mounted on motorized stage to move on a circular path in order to increase uniform coverage area. (Important for porous metal oxide films such as TiO ₂ where direct physical deposition occurs by evaporating solvent instead of pyrolysis)
Easy settings and operation	KV-25 can be controlled using on-board keypad and LCD or can be connected to a personal computer* through the USB port. (*personal computer is not included to the machine)

Utilities

Power supply and power consumption	100 VAC Single phase, 50/60 Hz, 1.5 kW or 240 VAC Single phase (on request)
Electrical standard	 
Air source pressure	Over 0.6 MPa (oil free air only, inlet: 6 mm ø)
Exhaust system	Built-in exhaust pump with powder filters. Exhaust outlet: 45 mm

Applications

Porous and dense thin film formation

- Transparent conducting oxide films (ITO, FTO, AZO etc.)
- Other functional films (TiO₂, ZnO, SnO₂, Cu₂O, SnS etc.)

Additional Features

- Automatic initializing (fill raw chemical in to tubes), draining (return raw chemical back to bottle), and cleaning.
- Up to 9 sets of different operation parameters (programs) storage capacity.
- Included a real time liquid flow monitoring system to display actual spray volume in each spray and total volume sprayed.
- Substrate and heater temperatures, atomizing air pressure are digitally displayed on the LCD. (Continuously monitor those parameters and give warning message if deviate from preset range.)
- Heater controlled by cascade PID controller with 2 temperature sensors. Five different set of PID value can be stored for different temperature regions.
- Built-in exhaust pump with input and output dust filters. (Exhaust air may contains chemical vapor that should go through a laboratory fume hood)

Home Page



SPD System

for thin film formation

KV-100



Specifications

Substrate size	Up to 100 mm × 100 mm
Substrate temperature	Max. 650 °C
Spray distance	150 mm to 250 mm (with ±0.1 mm accuracy)
Nozzle moving range	x-axis max: 150 mm, y-axis max: 150 mm
Reaction chamber	W320 mm x D360 x H360 mm with Teflon coating for corrosion resistance
External dimensions	W650 mm x D400 mm x H850 mm
Weight	85 kg
Capacity of solution bottle	250 ml

Special Features

Moving spray nozzle	Spray nozzle is mounted on motorized x-y stage and utilizes special spray line pattern to produce uniform film.
Spray rate control	Liquid-feeding-system of KV-100 equipped with an automated syringe pump allows user to set exact spray rate and total volume of liquid as initial parameters.
Remot control operation	Can be connected to a personal computer through an USB port and controlled all the functions remotely. Unlimited number of recipes can be saved with the computer.

Utilities

Power supply and power consumption	100 VAC single phase, 50/60 Hz, 1.5 kW
Electrical standard	 
Air source pressure	Over 0.6 MPa (oil free air only, inlet: 6 mm ø)
Exhaust system	Built-in exhaust pump with a dust filter for powder removal. Exhaust outlet: 50 mm

Applications

Porous and dense thin film formation

- Transparent conducting oxide films (ITO, FTO, ATO, AZO etc.)
- Other functional films (TiO₂, ZnO, SnO₂, Cu₂O, SnS etc.)

New Features

- Built-in exhaust pump with input and output dust filters. (Exhaust air may contain chemical vapor. External scrubber must be used to clean exhaust air)
- Easy setting of operation parameters using front panel keypad and LCD.
- Up to 9 sets of different film making recipes can be stored in the memory.
- Can be control remotely through a personal computer. (PC is not supplied as a part of the machine)
- Spray rate and volume in each spray, and total volume are displayed on LCD.
- Automatic initializing and ending functions: removes air from the tubes at the beginning and drain chemical at the end. Automatic cleaning function: assists user to clean the system.
- Substrate and heater temperatures, and atomizing air pressure are displayed on a separate LCD. (KV-100 continuously monitors those parameters and gives warning messages if deviate from preset range.)
- Heater is controlled by cascade PID controller with 2 temperature sensors. Five different sets of PID values can be stored for different temperature regions.

Home Page





SPD System

for thin film formation

KM-300

Specifications

Substrate size	Up to 300 mm × 300 mm
Substrate temperature	Max. 700 °C
Spray distance	250 mm to 350 mm
External dimensions	W2000 mm x D1200 x H1900 mm
Weight	Approximately 810 kg
Capacity of solution pod	1000 ml
Motion system	Closed-loop Servo Motors X-axis max : 525mm Y-axis max : 525mm
Movement speed of spray nozzle	150 mm/s Max.

Utilities

Power supply and power consumption	200 VAC Three phase, 50/60 Hz, 125 A
Air source pressure	150 NL/min, 0.5 MPa, Intake: Φ8 (oil free air only)
Exhaust system	Powder collection equipment: Cyclone separator Heat-resistant exhaust blower Exhaust outlet: 65 mm

Features

- Designed for substrates up to 300 mm by 300 mm. It utilizes three spray nozzles with special scanning pattern to reduce the overall coating time and produce highly uniform film.
- Largest coating area of 400 mm × 400 mm and multiple and orthogonal line-coatings.
- Detachable and washable inner walls of the reaction chamber, and also they are covered with ceramic coating films.
- Fully automatic operation with easy setting through touch sensing graphical operation terminal.
- Distance between the nozzle and substrate can be adjusted.
- Powerful ventilation of the downward flow and the cyclone powder separation system.
- Built-in exploded gas collection system.

Applications

Porous and dense thin film formation

- Transparent conducting oxide films (ITO, FTO, ATO, AZO etc.)
- Other functional films (TiO₂, ZnO, SnO₂, Cu₂O, SnS etc.)

Home Page





Preparation of Quality Transparent Conductive Oxides for Next Generation Solar Cells through a Spray Pyrolysis Deposition

Shun-ichi Ohta, P. V. Viraj Jayaweera and Shoji Kaneko

SPD Laboratory, Johoku, Hamamatsu 432-8011, Japan



Transparency of FTO on a glass substrate

Abstract

Homogeneous 150mm square FTO transparent electrode with 81.4% transmittance and 6.9 Ω/\square sheet resistance has been prepared by an intermittent spray pyrolysis deposition. The electrical properties of this film are proposed as follows: Resistivity $4.6 \times 10^{-4} \Omega\text{cm}$, Mobility 25.0 cm^2/Vs and Carrier Concentration $5.3 \times 10^{20}/\text{cm}^3$. Post-annealing effect on both physical properties was confirmed also.

I. Introduction

FTO has been used for perovskite solar cells as a transparent electrode, which are continuing to request the supply of quality FTO for performance improvement. A spray pyrolysis deposition (SPD) is one of chemical wet processes for thin film formation on a substrate. SPD is mostly carried out using double fluids of raw solution and compressed air at room temperature under an atmosphere, where gives tailored thin films from atomized raw material solutions using simple apparatus with easy operation. The spraying operation in our technology is done not consecutively but intermittently for suppressing remarkable reduction of a prescribed substrate temperature between 200 and 600, depending on the component and composition of thin film deposited [1-3].

II. Experimental

A starting solution containing raw materials is atomized intermittently to a heated substrate as droplets with compressed air, holding a prescribed substrate temperature. Because it takes several seconds to recover the substrate temperature after one shot of spray (Fig.1 and Table).

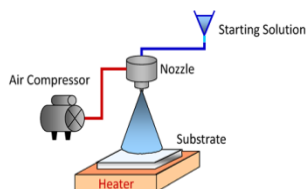


Fig.1. Spray Pyrolysis Deposition (SPD)

III. Results and Discussion

The coating of 150 mm square and 800 nm thick FTO with a visible light transmittance 81.4% and a sheet resistance 6.9 ohm/\square on 1.1 mm thick glass substrate was achieved by the above-mentioned SPD from a mixed ethanol solution including di- butyl tin (IV) di-acetate and ammonium fluoride after optimizing deposition conditions such as substrate temperature, intermittent time, rotation of substrate, nozzle moving velocity, and distance between nozzle and substrate. High quality of the FTO was assured also from small numerical deviations of transmittance and sheet resistance data measured at 36 different locations (Fig. 2).

Furthermore, we could obtain almost the same specifications of transmittance 81%, sheet resistance 7.1 ohm/\square and small deviation each in 300 mm square FTO (Film thickness 0.86 mm) after discussed on enlargement. It has been proved that our spray pyrolysis deposition is suitable for the preparation of quality transparent conductive FTO. The surface roughness and electronic properties of FTO obtained in this study will be discussed from AFM observation and Hall measurement, respectively (Figs. 3-5).

Film Thickness (nm)	Resistivity (Ωcm)	Carrier Concentration (cm^{-3})	Mobility (cm^2/Vs)	Sheet Resistance (Ω/\square)	Transmittance (%)
800	4.6×10^{-4}	5.3×10^{20}	25.0	6.9	81.4

References

- [1] I. Yagi and S. Kaneko, Chem. Lett., 1991, 156-9.
- [2] K. Murakami et al., J. Am. Ceram. Soc., 79 (1996) 2557-62.
- [3] E. V. A. Premalal et al., Thin Solid Films, 520 (2012) 6813-17.
- [4] L. Cojocaru et al., Chem. Lett., 44 (2015) 1750-52.

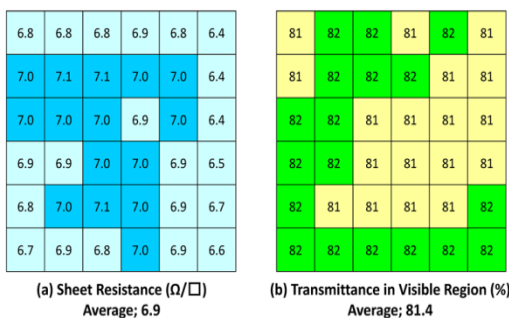


Fig.2. Sheet Resistance and Transmittance of FTO with 150 mm square

The surface roughness of FTO prepared here was smaller than a commercial product, but about half of the glass substrate (Fig. 3). The post-annealing processing of FTO caused to increase the sheet resistance over a temperature 700, and the transmittance over 600, both (Fig. 4), attributed to the surface roughness or grain growth of the film (Fig.5). The physical properties of FTO are summarized in Table.

Substrate Glass (Corning Eagle XG)	FTO (SPD)	FTO (SOLARONIX)
Roughness 0.7 nm	Roughness 6.1 nm	Roughness 11.3 nm

Fig.3. Surface Roughness of FTO

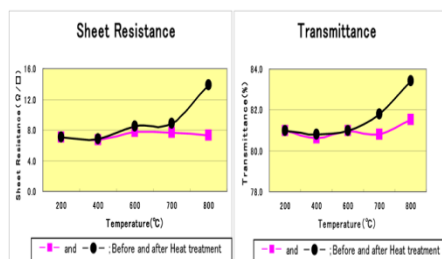


Fig.4. Post-annealing Effect of FTO on Sheet Resistance and Transmittance

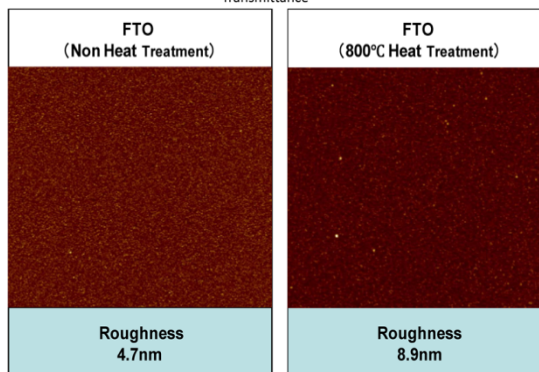


Fig.5. Surface Roughness of FTO



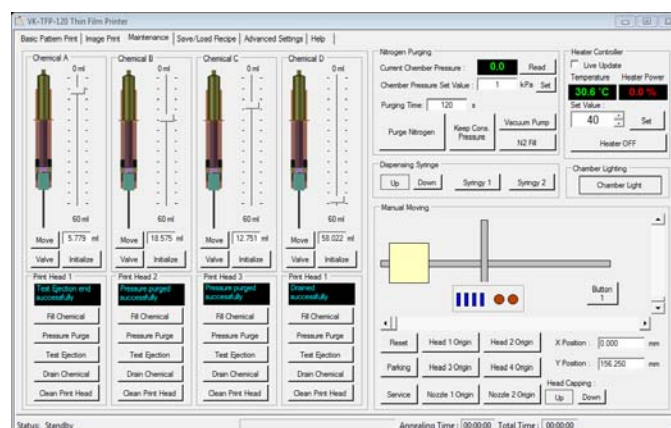
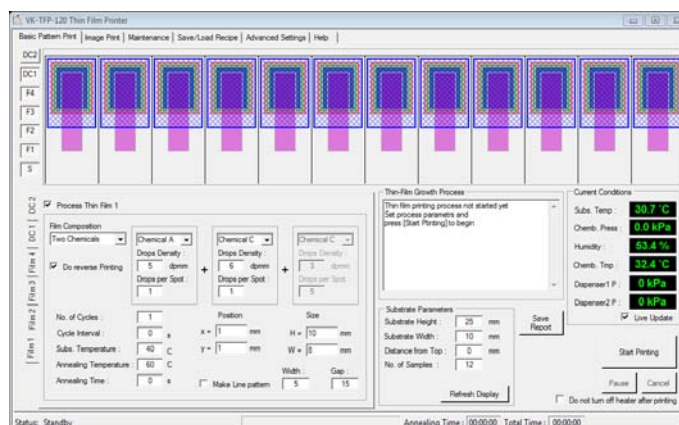
Inkjet Thin-Film Coater (with Paste Dispenser)

Model: VK-TFP-120



Specifications

Number of Printing Heads	4
Type of Print Head	Piezoelectric 128 nozzle, 80 pl/droplet, 16.5 mm print width
Number of Dispensing Nozzles	2 (ϕ 0.2 mm to 1 mm)
Maximum Printable Area	120 mm \times 120 mm
Substrate Temperature	RT – 155 °C
Printing Environment	Complete process perform in a nitrogen purge airtight chamber
Machine Control Method	Through the USB port using PC Software
Raw Materials	Up to 4 different chemical solutions for inkjet printing Up to 2 paste for dispense coating
Raw Material Inserting Method	Filled in to 60 ml Syringes
Dimensions	L 600 \times W 600 \times H 760 mm
Weight	50 kg



Special Features

Capability of making single or combined chemical film : Up to four different chemical solutions can be utilized to make single chemical or combined chemicals thin film formation by ink jet printing technique. Example: $\text{CH}_3\text{NH}_3\text{I}$ + PbCl_2 , Spiro-OMeTAD

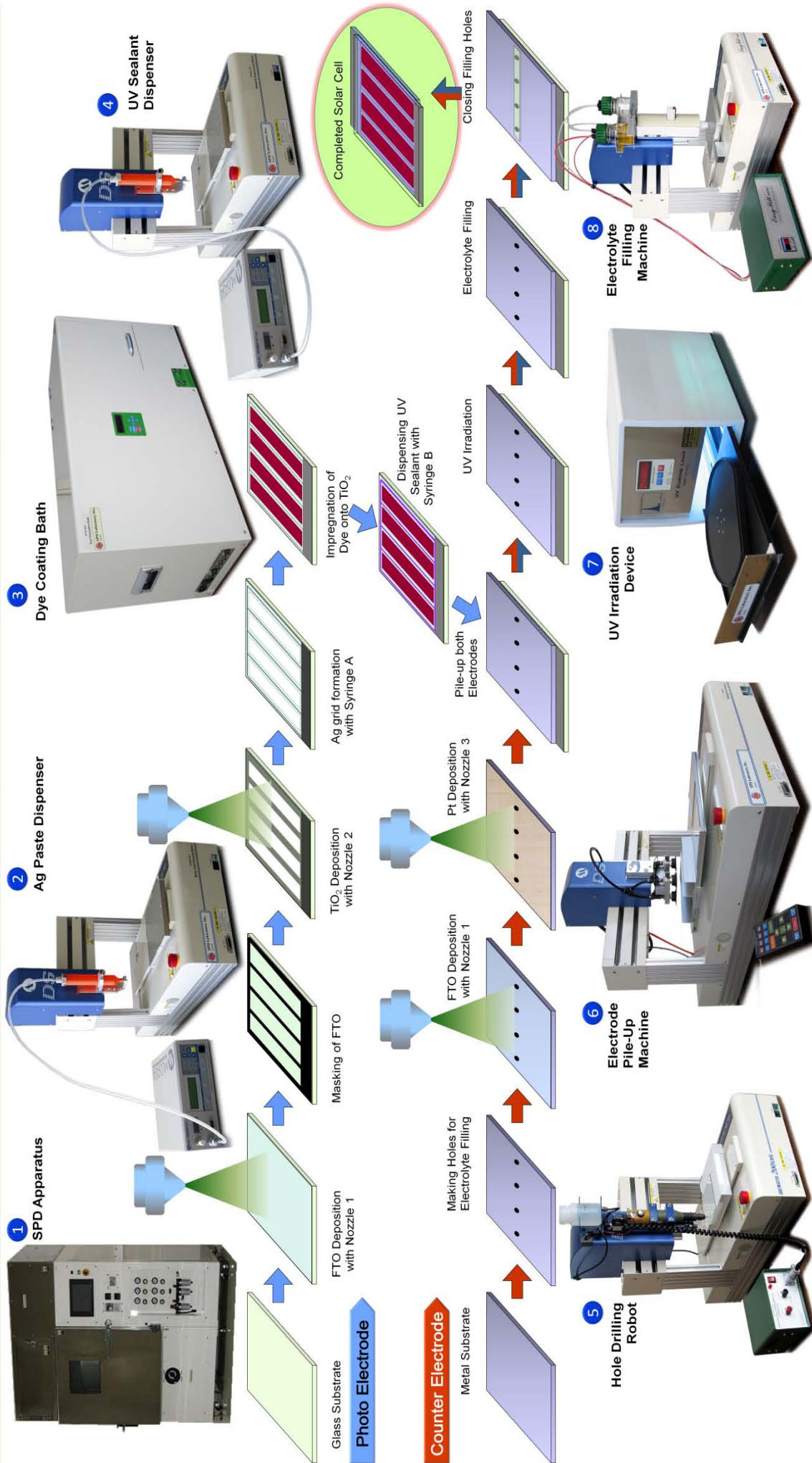
Capability of Paste Dispensing for Film Formation : Up to two different thick coatings can be dispensed with a single nozzle ($\Phi = 0.2 - 1$ mm). Example: Conducting carbon past, Encapsulating resin , Ag paste, etc.

Automatic Loading/Purging Function : Machine will automatically pump raw chemical solutions to the printing heads and remove air from the system.

Automatic Draining Function : This function will pump raw chemicals safely back to the storage syringes.

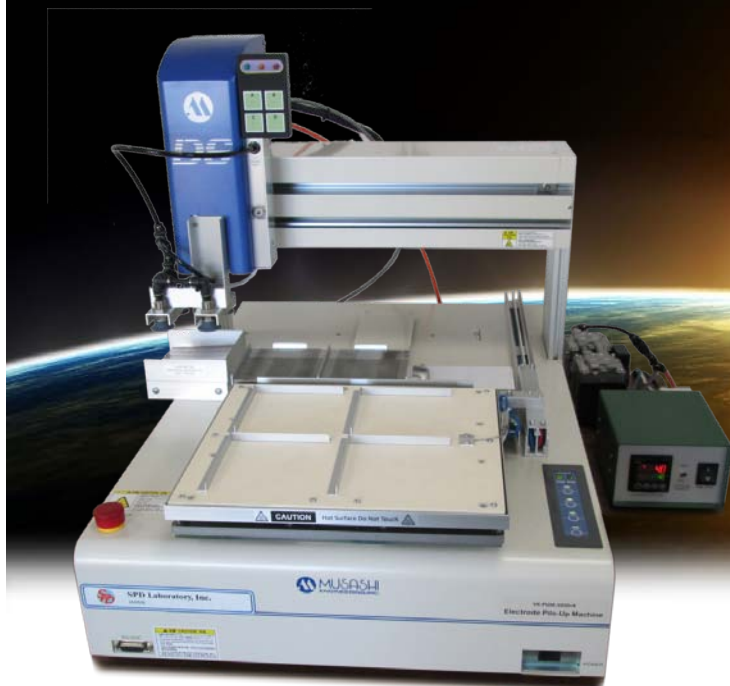
Automatic Cleaning Function : This function automatically cleans print heads and all tubing using a given chemical solution.

Fabrication Process of Large Area Dye-Sensitized Solar Cell Proposed by SPD Laboratory



Electrode Pile-Up Machine

Type: VK-PUM-1010×4



Home Page



Specifications

Loading method	Top electrodes: Automatically pick from the loading tray. About 135 sheets (assuming 0.2 mm thickness for a sheet) can be loaded to the tray. Bottom electrodes: Manually load on to the hotplate by user.
Unloading method	Automatically unload completed modules to the unloading tray. Tray can hold about 70 modules (assuming 0.4 mm thickness for a module). User should clear the tray before overflowing it.
Electrode pick-up method	Vacuum pads (4). Recommended maximum service temperature of rubber pads are 200°C. (Manufactures absolute maximum service temperature is 230°C)
Vacuum levels for weight blocks and flexible electrode sheets	For weight blocks: Full vacuum level of the pump For flexible electrodes: Vacuum level can be lower until electrode deformation disappear by rotating 2 flow-control valves.
Size of electrodes (mm)	100 × 100
Number of pile-up locations on the hotplate	4
Top electrode aligning method	Pre-determined position on the bottom electrode. (User can change the offset distance of 2 electrodes in the program)
Positioning accuracy of robot (μm)	±5
Weight block size (mm)	100 × 100
Weight block thickness	0.1 – 15 mm (User can change the value in the program)
Maximum weight of the block	1.2 kg
Supported electrode thicknesses (mm)	0.05 - 5
Normal operation temperature of hotplate	150 C
Maximum recommended hotplate temperature	200 C
PC interface (for modifying programs)	RS-232, (USB to RS-232 converter will be supplied)
Power Supply	100 V AC, 50/60 Hz
Dimensions (W × D × H) (mm)	500 × 710 × 568
Weight	31 kg

Automatic Electrolyte Filling Machine

EasyFill–master**Application:**

This machine automatically fills electrolyte into an enclosed cell with a single filling-hole. Filling hole position can be programmed to anywhere in the 150 mm x 150 mm sample holding table.

Features:

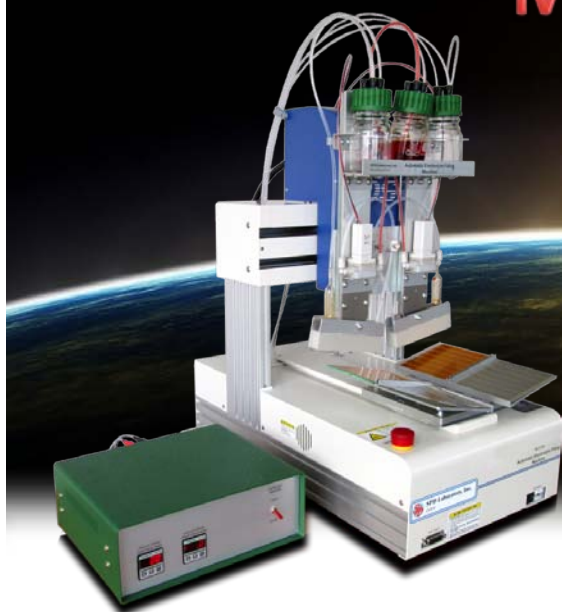
- Vacuum aided filling technique need only one hole for a cell.
- Filling process is completely under the N₂ (or other inert gas) atmosphere.
- Return step save the excess electrolyte in the filling head and tubs.
- The exposure time of electrolyte in to vacuum is minimized.
- Minimum usage of N₂ gas.
- Automatically adjust tip height for different thickness cells.
- Self cleaning process helps to wash and dry all the tubes and tip.

**Specifications:**

Maximum cell size (mm)	150 × 150
Filling Tip moving method	Automatic
Cell positioning method	Automatic
Automatic multi hole filling	Yes
Number of moving axis	X, Y, Z
Maximum moving range (mm)	200 (X, Y) 55 (Z)
Electrolyte bottle capacity (ml)	100
Rated Air Pressure (MPa)	0.6
Rated Vacuum level (mTorr)	100*
Control method	Computer Control*
PC interface	RS-232, USB
Control Software	EasyFill-2012-MA (Free of charge)
Vacuum Pump power ON/OFF	Automatic
Power Supply	100-240 V AC, 50/60 Hz
Dimensions (W × D × H) (mm)	304 × 304 × 422
Weight	14 kg

Automatic Electrolyte Filling Machine

Type: VK-EFM-1-7×2



- Fill 2 modules simultaneously
- No limitations for the number of cells in the module
- Filling rate: 2 modules/min
- Utilize vacuum aided filling technique
- Perform filling operation under N₂ environment
- Can be use for both flexible plastic modules and glass modules

Specifications

Filling Technique	Vacuum back filling. Need only one hole per cell.
Number of filling heads	2
Size of cell (mm)	100 × 100
Capacity of loading tray	4 cell modules. (2 modules will be filled simultaneously)
Filling speed	2 modules per minute
Rated Vacuum level (mTorr)	100
Vacuum pump	Single stage rotary oil pump
Electrolyte bottle capacity (ml)	100
Supported module thicknesses (mm)	0.5 - 5
Control method	Computer Control
PC interface	RS-232, USB
Control Software	EasyFill-2014-MCA (Free of charge)
Maximum recommended hotplate temperature	200 C
PC interface (for modifying programs)	RS-232, (USB to RS-232 converter will be supplied)
Power Supply	100 V AC, 50/60 Hz
Dimensions (W × D × H) (mm)	304 × 304 × 422
Weight	20 kg

Home Page



Perovskite Solar Cell (PSC) Preparation Process

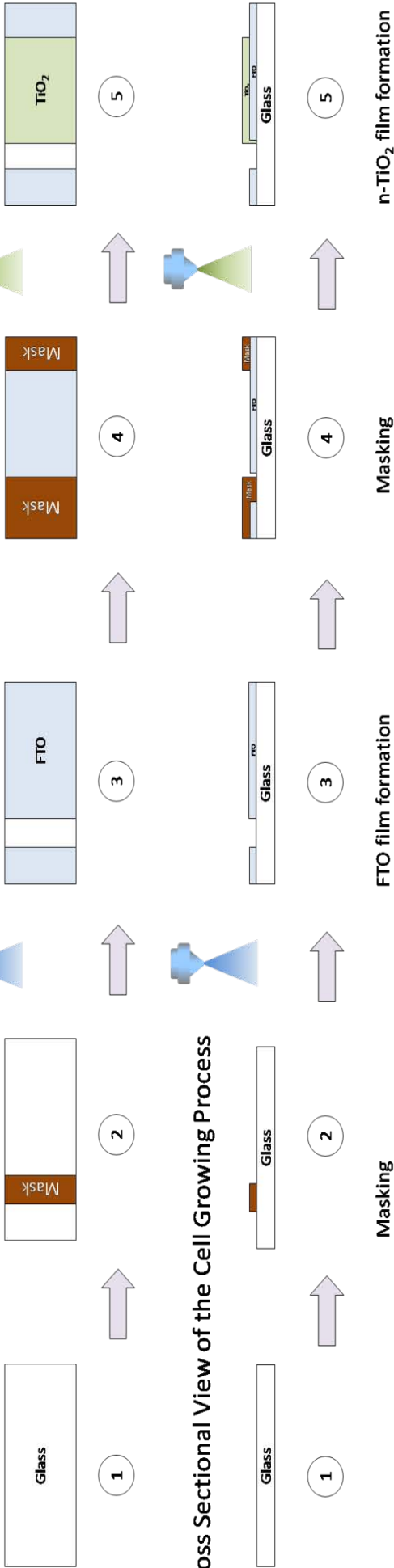
Proposed by SPD Laboratory, Inc.

Step 1: Patterned Transparent Conducting Oxide (TCO) Layer and TiO₂ (n-type Semiconductor) Layer Preparation by Spray Pyrolysis Deposition (SPD)

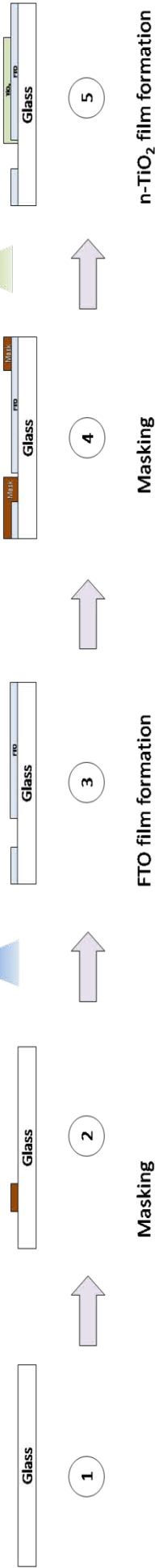


SPD Apparatus
KV-100

Top View of the Cell Growing Process

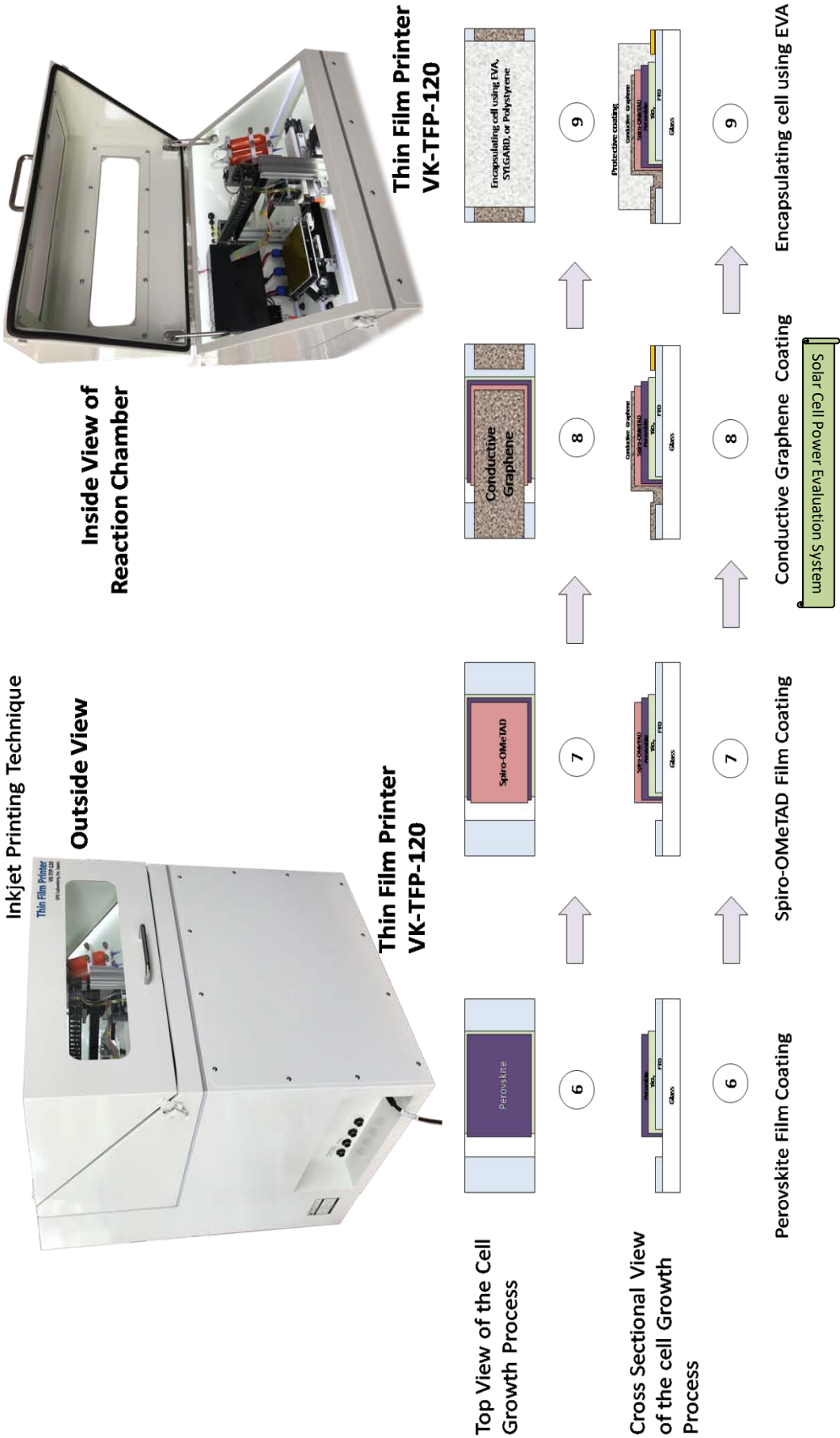


Cross Sectional View of the Cell Growing Process



Perovskite Solar Cell (PSC) Preparation Process Proposed by SPD Laboratory, Inc.

Step 2: Perovskite Layer ($\text{CH}_3\text{NH}_3\text{PbI}_3$), Spiro-OMeTAD (p-type Semiconductor) Layer and Back Contact Preparation by Piezoelectric Drop On Demand Inkjet Printing Technique





LED Solar Simulator

Type VK-SS-50

Innovative Solar Simulator Design Utilizing LED Light Sources

- Variable Output Adjustment from 0.0001 to 1.0 SUN
- User Settable Spectral Control
- Self Calibrating with Built-in Intensity Measurements
- More Than 20,000 Hours LED Lifetime
- Motorized sample mounting stage
- 30 mm × 30 mm Output Beam Size
- Energy Efficient Design



Home Page



Specifications

Simulator Class :

A (JIS C8912)

Independent LED Control :

Independently drives 22 LEDs spaced over the spectrum from 370 nm to 1030 nm

Spectral Matching:

Within $\pm 5\%$ of AM 1.5 G spectral characteristics in the range of 370 to 1030nm (at irradiance of 1000 W/m²)

Illumination Area and Distance:

30 mm × 30 mm
and 200 mm

Irradiation Intensity:

74 mW/cm² (integrated irradiance at 370 to 1030 nm)

Real-time Intensity Calibration :

Built-in calibrated Si photodiode allow user to perform intensity calibration anytime.



Illuminance Stability:	within $\pm 1\%$ / h (after 30 minutes of lighting)	Cooling method:	Forced air cooling
Illuminance Distribution:	within $\pm 5\%$ (within effective irradiation area of 25mm x 25mm) within $\pm 2\%$ (within effective irradiation area of 10mm x 10mm)	Irradiation Direction:	Downward irradiation
Software:	Communication with the PC by Bluetooth. The irradiation light spectrum can be adjusted by changing all 22 LEDs individually. It automatically adjusts to the set spectrum and measures the real output spectrum. Setting value recipes can be saved.	Motorized sample mounting stage:	Automatically select user sample and Si reference cell.
		Input voltage:	Single phase 100 V $\pm 5\%$ 50/60 Hz
		Dimensions:	400 × 400 × 550 mm (Lamp) 320 × 150 × 450 mm (control box)
		Weight:	~ 20 kg

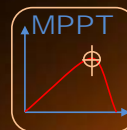
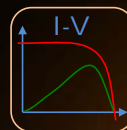


PV Power Analyzer

Type VK-PA-100

One Instrument for 5 Different Laboratory Applications:

- Solar cell I-V characterization (V_{OC} , J_{SC} , FF, η , R_s , R_{sh})
- Maximum Power Point Tracking with P_{max} & Efficiency vs. time plot
- Four quadrant I-V analysis (Dark I-V, Stepwise Cyclic Voltammetry)
- Four probe resistance measurements (Sheet resistance, Resistivity)
- Use as a potentiostat or Galvanostat



Specifications

Measurement Range (For details see page 3)	Voltage: ± 10 V Current: 1 A (3 A Pulse) with 5½-digits resolution
Measuring Technique	Digital Source Meter Type
Inputs	Front: 4 probes for PV device Back: 4 wire connector for reference cell (light intensity measurement)
A/D Converters	16 Bit (2 independent ADCs for V & I measurements)
User Interface and data collecting	Computer software is provided for control of all the functions and data logging. Measurement data can be saved as a text file and directly plotted on Microsoft Excel graph. (Windows based PC required)
Communication	Bluetooth wireless communication
Power Requirement	100 – 240 VAC (50-60 Hz)
Electrical standard	CE RoHS compliant
Dimensions, Weight	88 mm x 210 mm x 350 mm, 2.5 kg

Features of Solar Cell I-V Tracer

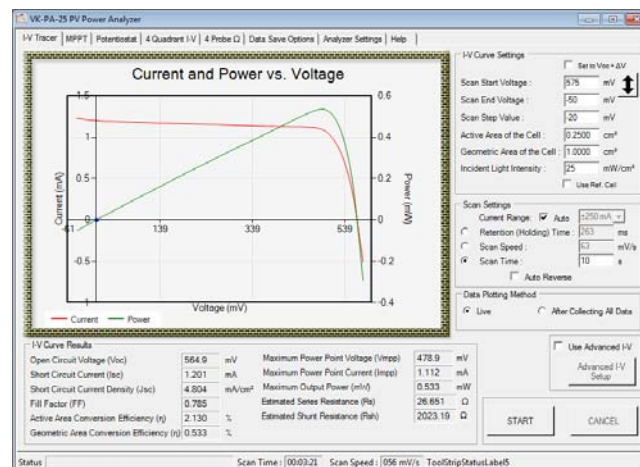
User selectable START, END and STEP voltages. Plots current and power vs. voltage curves. Calculated results include V_{OC} , I_{SC} , J_{SC} , P_{max} , V_{mpp} , I_{mpp} , FF, R_s , R_{sh} , η_{active} , and η_{geo} . User can set the desired scan speed, scan time, or holding time. Advanced I-V option allows initial, middle, and end point holding times. I vs. t transient plot for all data points and/or under a selected fixed voltage.

Features of Maximum Power Point Tracking (MPPT) Function

Analyzer acts like the best load for the cell to extract maximum power point (MPP) and keep tracking MPP continuously. Plots P_{max} , V_{mpp} , I_{mpp} and Efficiency vs. time curves and also display current/power vs. voltage plots.

Features of Potentiostat Function

Plot the current vs. time under a given fixed output voltage. User can directly measure the open circuit voltage, and short circuit current of the cell. Programmable electro deposit function.



Features of Full Range I-V Function

User selectable START, END, STEP voltages and SCAN SPEED (mV/s). Plot current vs. voltage curve for given number of voltage sweep cycles in potentiostat mode. Can be used in 3 electrodes liquid cell with reference electrode.

Four Probes Resistance Measurement

Three special functions included to easily measure **sheet resistance**, **resistivity**, and **resistance**. Geometric correction factors are automatically calculated according to size and measuring probe location on the sample which are entered as parameters. Measurement range 2.0×10^{-3} to $5.0 \times 10^6 \Omega$.



PV Power Analyzer

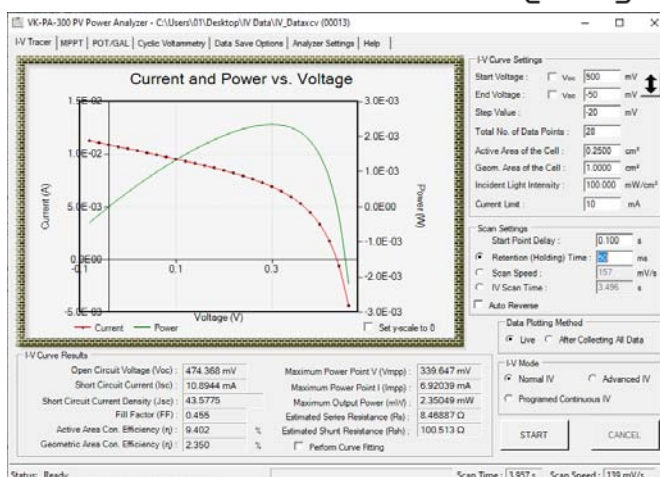
Type VK-PA-300

For I-V Tracing, Maximum Power Point Tracking, & Cyclic Voltammetry
The Measuring Range (up to 10V, up to 3A)



Specifications

Measurement Range (For details see page 4)	Voltage: ± 10 V Current: ± 1 A (± 3 A Pulse) with 5½-digits resolution
Measuring Technique	Digital Source Meter Type
Inputs	Front: 4 probes for PV device
A/D Converters	24 Bit (2 independent ADCs for V & I measurements)
User Interface and data collecting	Computer software is provided for control of all the functions and data logging. Measurement data can be saved as a text file (.csv or .txt) and directly plotted on Microsoft Excel graph. (Windows based PC required)
Communication	Bluetooth
Power Requirement	100 VAC (50-60 Hz)
Electrical standard	CE
Dimensions, Weight	260 mm(W) x 350 mm(D) x 133 mm(H), 6 kg



Features of Solar Cell I-V Tracer

User selectable START, END and STEP voltages. Plots current and power vs. voltage curves. Calculated results include V_{OC} , I_{SC} , J_{SC} , P_{max} , V_{mpp} , I_{mpp} , FF , R_s , R_{SH} , $\eta_{activeA}$, and η_{geoA} . User can set the desired scan speed, scan time, or holding time. Advanced I-V option allows initial, middle, and end point holding times. I vs. t transient plot for all data points and/or under a selected fixed voltage. Programmed Continuous IV" function allow user to take series of IV curves on given time intervals.

Features of Maximum Power Point Tracking (MPPT) Function

Analyzer acts like the best load for the cell to extract maximum power point (MPP) and keep tracking MPP continuously. Plots P_{max} , V_{mpp} , I_{mpp} and Efficiency vs. time curves and also display current/power vs. voltage plots.

Features of Potentiostat/Galvanostat Function

Plot the current vs. time under a given constant voltage or constant current. User can directly measure the open circuit voltage, and short circuit current of the cell.

Features Cyclic Voltammetry (CV)

Allows user to get both three electrode and two electrode CV plots for given voltage range, scan speed and number of cycles. This function mimics the analog triangle wave of voltage without digital voltage steps.



PV Power Analyzer

Type VK-PA-1000

**I-V Tracing and Maximum Power Point Tracking
for solar cell modules up to 100 V & 1 A
Comes with state-of-the-art control software**



Specifications

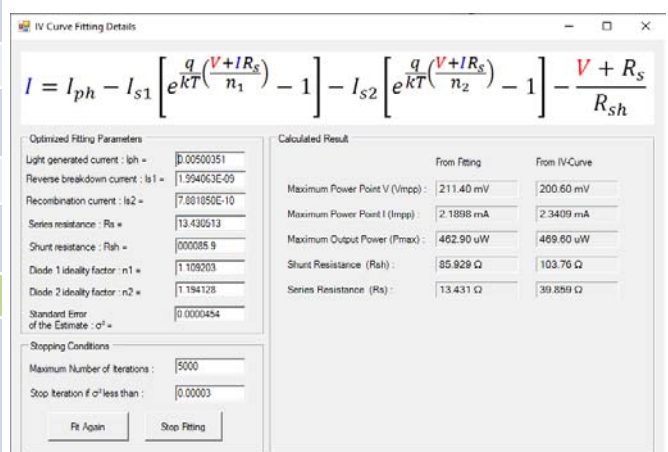
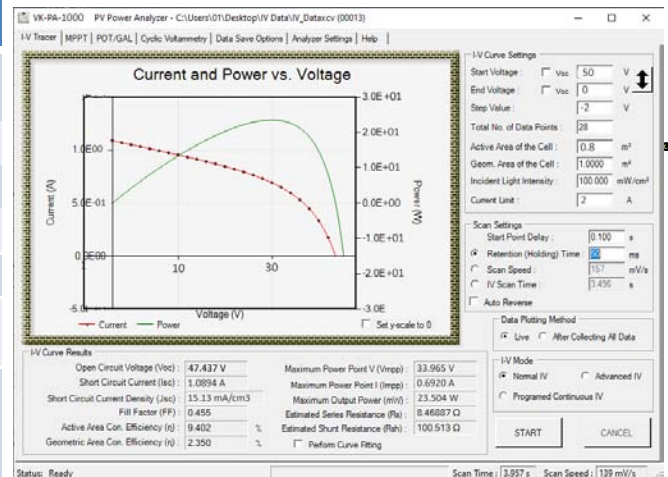
Measurement Range	Voltage: 100 V – 500 mV (8 Ranges) Current: 1 A – 50 uA (15 Ranges)			
Minimum Resolution (Max. 6½-digits)	Set		Measure	
	27 µV	1.5 nA	62 nV	12 pA
Measuring Technique	Electronic Load Type			
Inputs	Front: 4 probes for PV device			
A/D Converters	24 Bit (2 independent ADCs for V & I measurements)			
User Interface and data collecting	Computer software is provided for control of all the functions and data logging. Measurement data can be saved as a text file (.csv or .txt) and directly plotted on Microsoft Excel graph. (Windows based PC required)			
Communication	Bluetooth			
Power Requirement	100 VAC (50-60 Hz) 230 VAC (50-60 Hz)			
Electrical standard				
Dimensions, Weight	260 mm(W) x 350 mm(D) x 133 mm(H) , 5 kg			

Features of Solar Cell I-V Tracer

User selectable START, END and STEP voltages. Plots current and power vs. voltage curves. Calculated results include V_{OC} , I_{SC} , J_{SC} , P_{max} , V_{mpp} , I_{mpp} , FF , R_s , R_{SH} , $\eta_{activeA}$, and η_{geoA} . User can set the desired scan speed, scan time, or holding time. Advanced I-V option allows initial, middle, and end point holding times. I vs. t transient plot for all data points and/or under a selected fixed voltage. "Programmed continuous I-V" function allows user to take series of IV curves on given time intervals. Dedicated I-V curve fitting function included to the control software.

Features of Maximum Power Point Tracking (MPPT) Function

Analyzer acts like the best load for the cell to extract maximum power point (MPP) and keep tracking MPP continuously. Plots P_{max} , V_{mpp} , I_{mpp} and Efficiency vs. time curves and also display current/power vs. voltage plots.






Multi-Channel PV Power Analyzer

Type VK-MPA-100

- I-V Tracing and Maximum Power Point Tracking (MPPT) up to 6 solar cells simultaneously
- Continuously plot light intensity & temperature data along with P_{max}
- Each sample can have a capacity up to 10 V & 1 A
- Comes with dedicated user friendly control software
- State-of-the-art wireless communication with PC software



Specifications

Number of Channels	PV devices	light intensity Measurements		Temperature Measurements (K-type)	Auxiliary Outputs	
		Photodiode	Pyranometers		Relay Output (10A)	Open Drain
		6	1	3	1	1
Measurement Range	Voltage: 10 V – 120 mV (5 Measuring Ranges) Current: 1 A – 20 uA (16 Measuring Ranges)					
Maximum Resolution (Max. 6½-digits)	Current		Voltage		Voltage Setting	
	3 pA		16 nV		162 μV	
Measuring Technique	This analyzer consists of 6 independent programmable-electronic-loads. Simultaneous I-V tracing is possible. During MPPT measurements, each sample is separately maintained at its maximum power point by the MPPT algorithm in the microcontroller firmware.					
Light Intensity Measurement	Incident light intensity and temperature data are continuously obtained during I-V tracing and MPPT measurements. <u>Si Photodiode Port</u> : The analyzer has a built-in trans-impedance amplifier to measure the short circuit current of calibrated Si photodiode. Si photodiode (Hamamatsu Photonics) is provided with the system. Also, customer can use their own photodiode after modifying the calibration constant value in the “Advanced Settings” section of the software. <u>Pyranometer Port</u> : Up to 3 pyranometers can be connected as the light measuring sensors.					
Sample Connecting Ports	Six set of 4-wire connectors for samples					
A/D & D/A Converters	Two separate 24-bit ADCs for simultaneous voltage and current measurements. Six separate 16-bit DACs for setting cell voltages. Light Intensity data is measured using 24-bit ADC					
Control Software	Dedicated user-friendly computer software is provided to control all of the functions and data logging. Measurement data can be saved as a text file (.csv or .txt) and directly plotted as a *Microsoft Excel graph. The customer should prepare a Windows-based PC (with Bluetooth) to install this control software. (If you wish to have a new laptop PC, you can order as a separate option from us)					
Communication	Measured data wirelessly transfer to PC through Bluetooth for visualize on graphs.					
Power Requirement	100 VAC (50-60 Hz) 2A , 230 VAC (50-60 Hz) 1A			Electrical Standard	CE	
Dimensions, Weight	320 mm(W) x 450 mm(D) x 150 mm(H) , ~8 kg					

Features of Solar Cell I-V Tracing Function

Up to 6 solar cells can be connected to the analyzer. User selectable START, END and STEP voltages. Plots current and power vs. voltage curves. Calculated results include V_{oc} , I_{sc} , J_{sc} , P_{max} , V_{mpp} , I_{mpp} , FF , R_s , R_{sh} , $\eta_{activeA}$, and η_{geoA} . User can set the desired scan speed, scan time, or holding time. Advanced I-V option allows initial, middle, and end point holding times. I vs. t transient plot for selected data points under a selected fixed voltage. “Programmed continuous I-V” function allows user to take series of IV curves with given time intervals. Incident light intensity data also measured during I-V and used to calculate power conversion efficiencies. Also, the control software includes dedicated I-V curve fitting function.

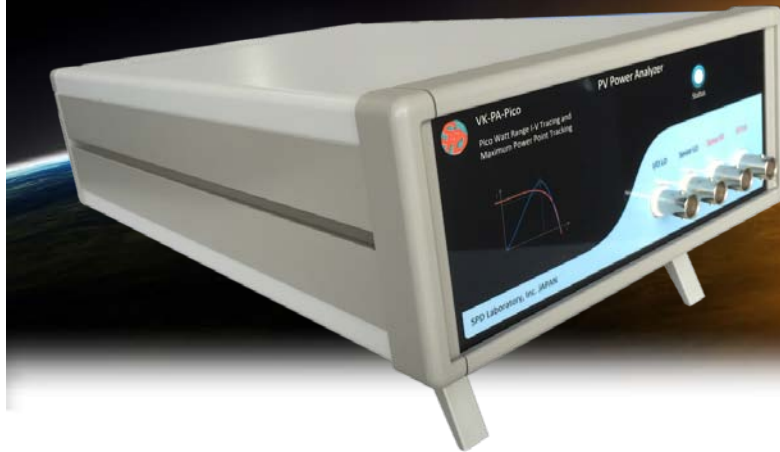
Features of Maximum Power Point Tracking (MPPT) Function

The analyzer search for each cell's maximum power point (MPP) and keep tracking MPP continuously. Control software plots P_{max} , V_{mpp} , I_{mpp} , and conversion efficiency vs. time curves for all connected cells with the light intensity. Also display current/power vs. voltage plots for each cell in a separate graph.

PV Power Analyzer

Type VK-PA-Pico

For Pico Ampere Range I-V Tracing and
Pico Watt Range Maximum Power Point Tracking (MPPT)



Specifications

Measurement Range	Voltage: ± 10 V Current: Max. ± 5 mA, Min. 10 pA
Current Measuring Ranges	<div> ± 5 mA (resolution 160 nA) ± 2.5 mA (resolution 80 nA) ± 1.25 mA (resolution 40 nA) ± 600 μA (resolution 20 nA) ± 300 μA (resolution 10 nA) ± 120 μA (resolution 4 nA) ± 60 μA (resolution 2 nA) ± 30 μA (resolution 1 nA) ± 15 μA (resolution 500 pA) ± 7 μA (resolution 250 pA) ± 3.5 μA (resolution 100 pA) ± 1.8 μA (resolution 60 pA) </div> <div> ± 900 nA (resolution 30 pA) ± 450 nA (resolution 15 pA) ± 230 nA (resolution 7 pA) ± 115 nA (resolution 4 pA) ± 55 nA (resolution 2 pA) ± 35 nA (resolution 1 pA) ± 18 nA (resolution 0.6 pA) ± 9 nA (resolution 0.3 pA) ± 4 nA (resolution 0.1 pA) ± 2 nA (resolution 70 fA) ± 1 nA (resolution 35 fA) ± 600 pA (resolution 17 fA) </div>
User Interface and Data Collection	Computer software is provided for control of all the functions and data logging. Measurement data can be saved as a text file and directly plotted on Microsoft Excel graph. (Windows based PC required)
Communication	USB
Power Requirement	100 – 240 VAC (50-60 Hz)
Dimensions, Weight	210 mm (W) x 350 mm (D) x 88 mm (H) , 3.0 kg



Pico Ammeter

In this mode, analyzer works as an Ideal ammeter (voltage drop < 5 μ V) to measure short circuit current of solar cell.

Potentiostat

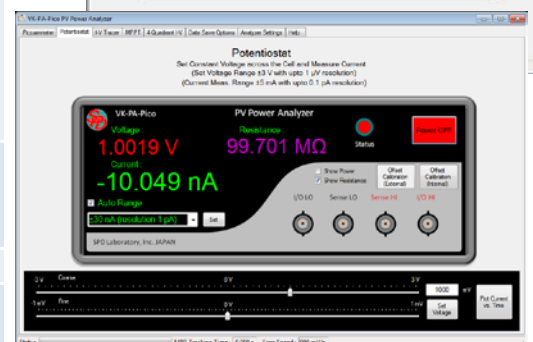
In this mode, analyzer measures current under a constant voltage given by user. Voltage, Current, Power or Resistance is displayed onscreen. It is also possible to plot those parameters against time.

I-V Tracer

In this mode, user can select START, END, and STEP voltages and scan condition (desired scan speed, scan time, or holding time). Analyzer plots current and power vs. voltage curves. Calculated results include V_{OC} , I_{SC} , J_{SC} , P_{max} , V_{mpp} , I_{mpp} , FF, R_{S} , R_{SH} , $\eta_{activeA}$, and η_{geoA} . Advanced I-V option allows to set initial, middle, and end point holding times. Also plots I vs. t transient curve for all data points and/or under a selected fixed voltage.

Maximum Power Point Tracking (MPPT)

In this mode, analyzer acts like the best load for solar cell to extract maximum power and keep tracking MPP continuously. Plots the P_{max} , V_{mpp} , I_{mpp} and Efficiency vs. time curves and also displays current/power vs. voltage plots.



Home Page





Capacitance Analyzer

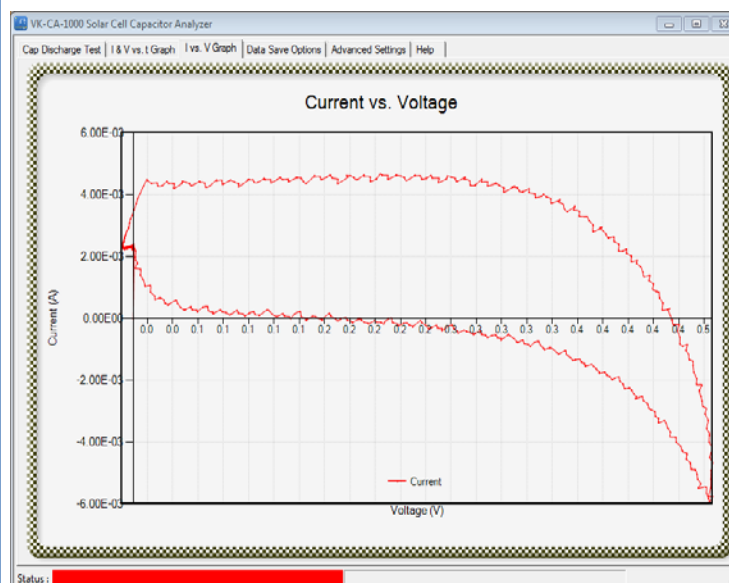
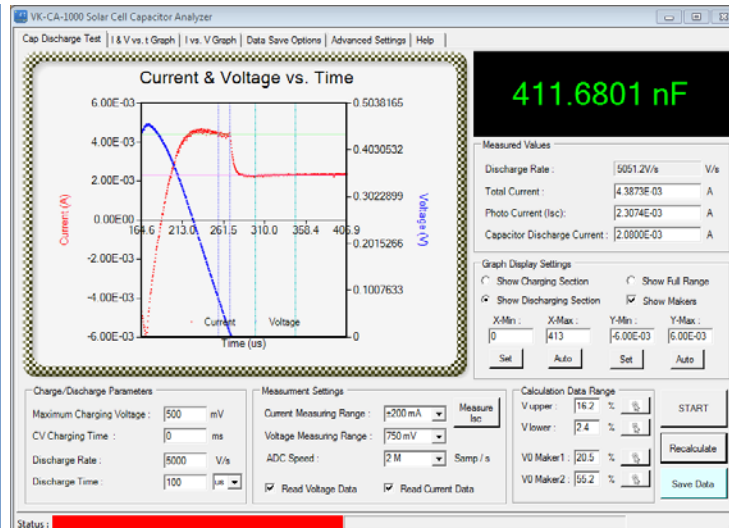
Type: VK-CA-1000

- Utilized DC charge-discharge technique with pico-second resolution time measurements
- Measurement range 1 pF to 1 F
- Automatic range selection
- User configurable discharge voltage limits



Specifications

Measurement Range and Accuracy	1pF - 1 nF with 1% accuracy 1nF - 1F with 0.6% accuracy
Measuring Technique	Based on discharge time measurement of RC circuit for two given voltage levels. Time measurements perform using precision timer with 217 ps resolution. Instrument continuously calibrating against known capacitors to eliminate stray capacitance and propagation delays in the electronic circuits.
User Configurable Parameters	Maximum charging voltage (0.5 – 3.3 V) Upper and lower voltage levels for discharge time measurement
User Interface and data collection	Computer software is provided for control of all functions and data logging. Measurement data can be saved as a text file and directly plotted on [®] Microsoft Excel graph. (Windows based PC required)
Communication	Bluetooth
Power Requirement	100 – 240 VAC (50-60 Hz)
Electrical standard	
Dimensions, Weight	210 mm (W) x 350 mm (D) x 88 mm (H) ~3.0 kg





Capacitor and Battery Analyzer

Type: VK-CA-8000



- Specially designed for electric-double layer capacitors (EDLCs), battery, and solar cell research
- Source and measure up to 20V and 10A
- Versatile control software provides all necessary data analyzing tools with automated curve fitting to evaluate capacitance, power, energy of EDLCs, and capacity, cycles life testing of batteries.
 - Constant current charge-discharge test
 - Cyclic voltammetry curve
 - Self discharge analysis etc...
- Can be used as a potentiostat or a galvanostat with 4 probes



Home Page



Specifications

Measurement Range	Max. Voltage: 20 V Max. Current: 10 A (pulse) 8 A (continuous) with 5½-digits measuring resolution
Measuring Technique	Digital Source/Measure Unit
Inputs	Front: 4 probes
A/D Converters	24 Bit (2 independent ADCs for V & I readings) up to 30,000 SPS
User Interface and data collection	Computer software is provided for control of all functions and data logging. Measurement data can be saved as a text file and directly plotted on ®Microsoft Excel graph. (Windows based PC required)
Communication	Through a USB port
Power Requirement	100 – 240 VAC (50-60 Hz)
Electrical standard	 
Dimensions, Weight	320 mm(W) x 450 mm(D) x 150 mm(H), 10 kg

Built-in Software Features

For EDLCs Analysis:

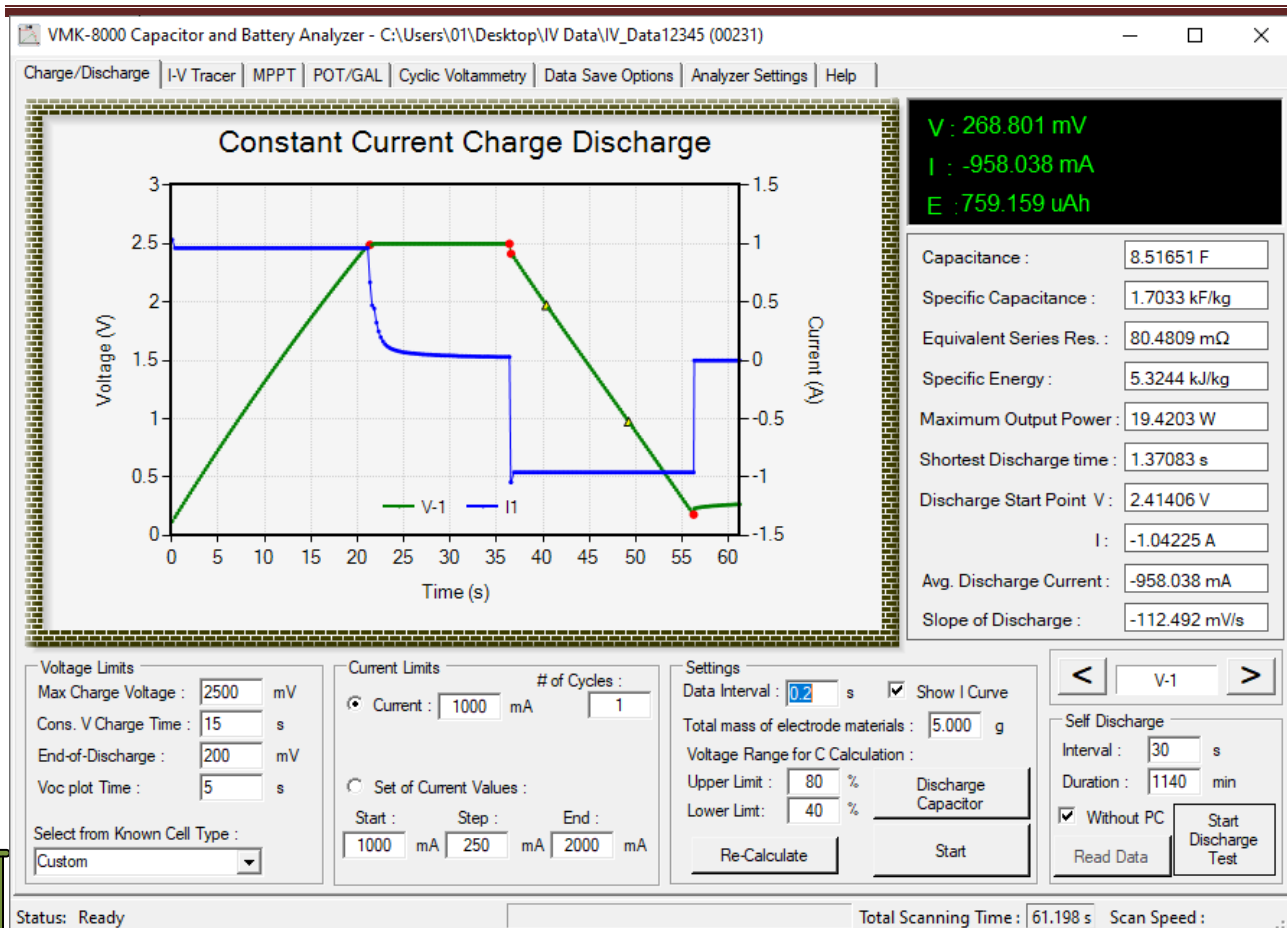
- ✓ Measurement of constant current charge-discharge test with given voltage compliance.
- ✓ Plot cyclic voltammetry curve
- ✓ Curve fittings for ideal RC model and nonlinear real model R-CPE(Q, α).
- ✓ Calculation of energy vs. time plots
- ✓ Calculation of energy vs. power curve
- ✓ Self discharge analysis
- ✓ Cycle life testing

For Battery Analysis:

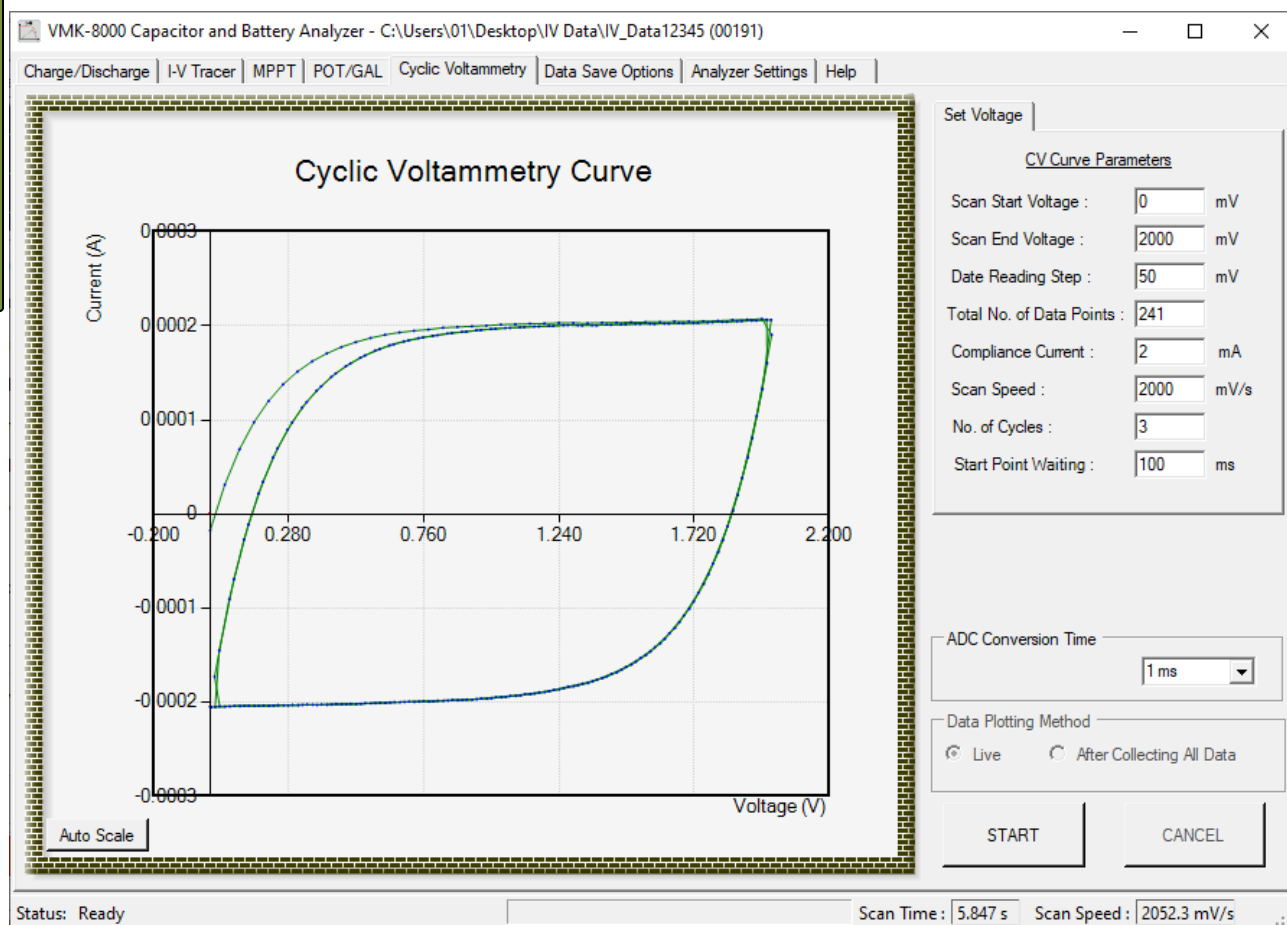
- ✓ Measurement of constant current charge-discharge curve with given voltage compliance.
- ✓ Analysis of both charge and discharge data
- ✓ Self discharge analysis
- ✓ Cycle life testing
- ✓ Limit based analysis (voltage, current, temperature, ohmic value)

General capabilities:

- ✓ I-V tracing for solar cell
- ✓ Use as potentiostat with 4 wires
- ✓ Use as galvanostat
- ✓ 4-probe resistance measurement
- ✓ Use as lead-acid, Li-ion, Li polymer battery charger up to 8A and 20 V
- ✓ All data and graphs can be directly save as ®Microsoft Excel files
- ✓ All measurement parameters can be saved and reload when needed to repeat at the same experiment



Screenshot of Charge/Discharge tab



Screenshot of Cyclic Voltammetry (CV) tab



IPCE & Spectral Response Measurement System

Type: VK-IPCE-10

- This compact instrument with fully automatic operation allows user to perform IPCE measurement by one click.
- User-friendly simple operation interface allows to start measurement quickly without reading bulky manuals and setting up various parameters.
- State-of-the-art Bluetooth communication allows user to control all the functions remotely.
- No attached equipments such as lock-in amplifier, source meter, and lamp power supply, only the main power switch needs to turn on.
- Utilize 100 % Digital Signal Processing (DSP) technique with Fast Fourier Transform (FFT) to measure synchronous current produced with chopped light beam.
- The double beam technique with a Si reference cell measures sample current & light intensity simultaneously.
- The motorized sample mounting stage aligns sample precisely.



Specifications

Type of Measurement	Incident Photon-to-electron Conversion Efficiency (IPCE), Spectral response (A/W)
Wavelength Range	340 - 1000 nm (calibrated photo diode limits) 0 - 1400 nm mechanical limit
Light Source	Halogen Photo Optic Lamp (OSRAM XENOPHOT®) 3400 K. Life time of Halogen lamp is greatly enhanced due to variable power operation technique where lamp is operated at less than half of rated power.
Irradiation modes	Natural (Halogen lamp spectrum) Constant energy Constant photon (Constant energy or photon Irradiation mode is achieved by controlling the halogen lamp current. Automatic calibration process performs the calibration of lamp current to keep constant energy or photon output).
monochromatic light power on sample	1 to 100 μ W (400 - 1000 nm range)
Measuring technique	Optically chopped (1 – 21 Hz) light beam is split into two parts (double beam technique) then incident on Device-Under-Test (DUT), and calibrated Si reference (REF) cell. Simultaneously digitized DUT and REF signals (short circuit currents) were Fast Fourier Transform (FFT) to obtain power spectrum (filter out only the chopped frequency component).
Grating	1200G/ 500nm blaze
Filters	Up to 5 different high-order light cut filters can be installed. L-37 and R-64 installed.
Recommended sample size	10 mm x 10 mm
White light (bias) source	Three watts white LED (output power can be set through the software).
Sample mounting stage	This system equipped with motorized sample mounting stage. User can remotely switch the sample and standard Si photo diode in order to do baseline calibration or verify accuracy of measurements.
User Interface and data collecting	Computer software is provided free of charge to control all of the functions and data logging. Measurement data can be saved as a text file and directly plotted on [®] Microsoft Excel graph. User interface is designed such that normal user can be performed measurements by setting just the scan wavelength range. Also advanced user can control hardware settings such as grating and filter changing position FFT bin size and also able to get raw I vs. t and FFT data.
Communication	Bluetooth
Power Requirement	100 – 240 VAC (50-60 Hz) Input voltage selection switch available to set the correct input voltage range.
Dimensions Weight	91 cm x 47 cm x 29 cm, 20 kg
PC	Windows based PC is needed to install control software, despite not included to the standard setup and can be added as a option.



Power Management Board for Energy Harvesting Applications

Type (1)
VK-PM-5V

INPUT: 130 mV to 3 V

Ex. Solar cell
TE Generator
Supercapacitor

VK-PM-5V

PFM Boost
Converter
& Battery
Management

OUTPUT: 2.5 V to 5.25 V

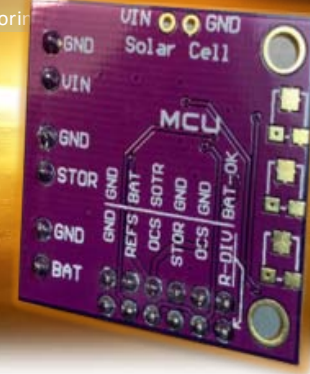
Fixed V as your requirement
Ex. LED Lighting
Wireless Sensors
Environmental Monitoring

STORAGE : (optional)
2.5 V to 5.25 V

Ex. Li Battery
Supercapacitor

Applications:

Solar Chargers
Thermal Electric Generator (TEG) Harvesting
Wireless Sensor Networks (WSN)
Low Power Wireless Monitoring
Environmental Monitoring
Bridge and Structural Health Monitoring (SHM)
Smart Building Controls
Portable and Wearable Health Devices
Entertainment System Remote Controls



Home Page

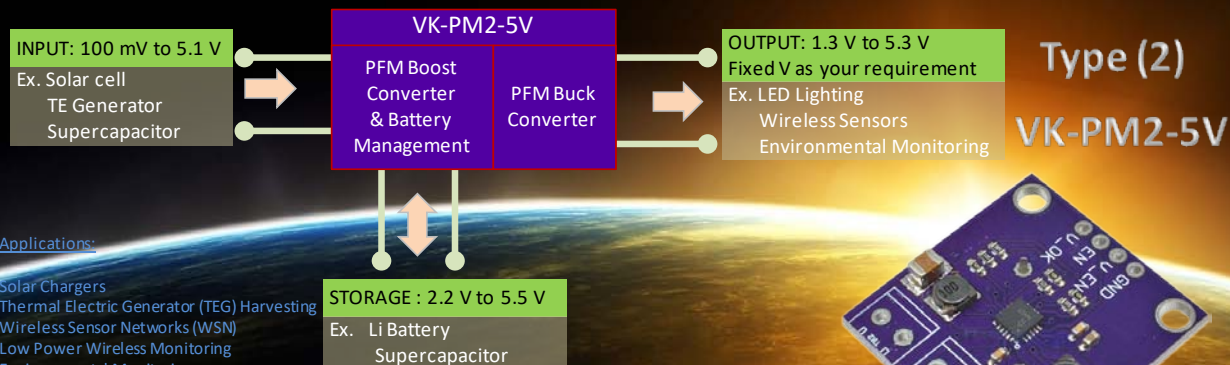


Specifications

Description	The circuit board is designed to collect and manage microwatt (μW) to milliwatt (mW) power generated from various DC sources such as photovoltaic (solar) cells or thermoelectric generators. This unit implements a high efficiency boost converter/charger for products and systems with tight power and operational requirements. This DC-DC boost converter/charger requires only microwatts of power to start working.
Characteristic	<ul style="list-style-type: none"> Ultra Low Power, High Efficiency DC-DC Boost Converter/Charger Continuous energy harvesting from low voltage input supply: $V_{IN} \geq 130\text{mV}$ Ultra-low quiescent current: $I_Q < 330\text{nA}$ (typical) Cold start voltage: $V_{IN} \geq 600\text{mV}$ (typical) Programmable Dynamic Maximum Power Point Tracking (MPPT).
Energy source input voltage	0.13V - 3V (Cold start voltage is 600 mV) It will continue energy harvesting from V_{IN} as low as 130 mV
Energy storage component and Voltage	2.5 V - 5.25 V Energy can be stored to rechargeable li-ion battery, thin-film battery, super-capacitor, or conventional capacitor. By default unit is set to 3.1 V. Please request us if you need different storage voltage.
Working environment temperature	-40 ~85 °C
Boost mode switching frequency	up to 1MHZ
Working mode	cold start mode, boost mode, thermal protection cut-off mode
Example input sources	Solar cell, thermo electric generator, micro wind generator etc...



Power Management Board for Energy Harvesting Applications



Applications:

Solar Chargers
Thermal Electric Generator (TEG) Harvesting
Wireless Sensor Networks (WSN)
Low Power Wireless Monitoring
Environmental Monitoring
Bridge and Structural Health Monitoring (SHM)
Smart Building Controls
Portable and Wearable Health Devices
Entertainment System Remote Controls

Home Page



Specifications

Description	The circuit board is designed to collect and manage microwatt (μW) to milliwatt (mW) power generated from various DC sources such as solar cells or thermoelectric generators. In addition to the highly efficient boosting charger, this board includes a highly efficient nano- power buck converter in the output stage. A supercapacitor (0.22F 5.5V) is installed onboard as a storage.
Characteristic	<ul style="list-style-type: none"> Ultra Low Power, High Efficiency DC-DC Boost Converter/Charger Programmable step down regulated output Buck Converter Continuous energy harvesting from low voltage input supply: $V_{IN} \geq 100 \text{ mV}$ Full operating quiescent current: 488 nA (typical) Cold start voltage: $V_{IN} \geq 600\text{mV}$ (typical) Programmable Dynamic Maximum Power Point Tracking (MPPT)
Energy source input voltage	0.1V – 5.1V (Cold start voltage is 600 mV) It will continue energy harvesting from V_{IN} as low as 100 mV
Energy storage component and Voltage	0.22 F, 5 V Supercapacitor mounted onboard Energy can be stored to rechargeable li-ion battery, thin-film battery, super-capacitor, or conventional capacitor. Voltage range is 1.3 V - 5.3 V (Can be set to your voltage requirement)
Working environment temperature	-40 ~85 °C
Switching frequency	Boost charger up to 1MHZ, Buck converter up to 500 kHz
Working mode	Cold start mode, boost mode, thermal protection cut-off mode
Example input sources	Solar cell, thermo electric generator, micro wind generator etc...



High-Resolution Wireless Data Logger

Features:

24-bit ADC Resolution
Up to 7 channels voltage data collection capability
Up to 30,000 samples per second conversion rate
Seven different measuring ranges 5 V ... 78 mV
Wireless Bluetooth communication

VK-DL-1256



Specifications

Description	This unit can read up to 7 channels of voltage (with 24-bit resolution) and wirelessly transfer to PC software for display & plot. Also there are several programmable digital and analog output channels available to control external devices. This unit comes with user friendly control software and can be integrated with SPD Lab PV Power Analyzers, and capacitor and Battery Analyzer.						
Voltage Ranges	5 V	2.5 V	1.25 V	625 mV	312 mV	156 mV	78 mV
Voltage Reading Resolution	298 nV	149 nV	74 nV	37 nV	19 nV	9 nV	5 nV
Number of Analog Input Channels	7						
Data Conversion Rate (SPS)	Maximum 30,000 samples per second						
Input Impedance	80 MΩ (<50 SPS), 10 MΩ (>2000 SPS)						
Temperature coefficient of internal voltage reference	±20 ppm						
Analog to digital conversion resolution	24-bit						
Number of trigger Input (0 - 3.3V)	1 (voltage data reading can be synchronize with this input)						
Optional digital input/output	Customizable up-to 20 digital input output						
Control Software	Data logger control software is supplied with the system (can be integrated to VK-PA series and VK-CA series analyzer software)						
Communication method with PC	Bluetooth						
Power supply	DC 5V (AC adaptor is supplied)						
Dimension	W 5 cm D 18cm, H 7 cm						
Weight	~350 g						

[Home Page](#)




Remote Switching System

VK-SW-16



Specifications

Description	This unit consist of 16 2-way switches (relay) that can use to switch up to 10 A of current. Individual outputs of all 16 switches are available for user to wire as their requirement. Each switch can be control through the software wirelessly (Bluetooth). This unit comes with user friendly control software and can be integrated with SPD Lab PV Power Analyzers, and capacitor and Battery Analyzer.
Number of channels	16
Maximum load current	10 A
Control Software	Switching system control software is supplied with the system (can be integrated to VK-PA series and VK-CA series analyzer software)
Communication method with PC	Bluetooth
Power supply	DC 12V (AC adaptor is supplied)
Dimension	W 5 cm D 18cm, H 7 cm
Weight	~350 g

Switching System



Four Probe Station

Type VK-PS-100

- ❖ For sheet resistance , resistivity measurements
- ❖ Customizable tip shapes , gaps, and arrangements
- ❖ Excellent repeatability



Specifications

Four Probe Arrangement	Linear or Square (or as requested by customer)
Probe Gap	Customizable (minimum gap 1.6 mm)
Tip Height Adjustment	5 mm fine movement with side hand lever Table top to tip distance can be set (by rotating top knob) from 10 - 100 mm
Tip shapes	Customizable with one of following available tip shapes
	<p>A photograph showing several different probe tip shapes (linear, square, and circular) arranged vertically next to a ruler with a 0.5 mm scale.</p>



Sample Holder

for electrical connections

Type VK-SH-150



- ❖ Four spring tensioned electrical contact probes
- ❖ Ideal for I-V, CV, or capacitance measurements
- ❖ Independently adjustable probe positions
- ❖ Customizable sample holder for different size samples

Specifications	
Table size	150 × 150 mm
Sample size	Customizable
Number of contact probes	4 in standard model, can be increased if requested
Sample mounting method	Easy retraceable sample mounting block with 4 magnets 
Contact Probe position	Each contact probe position can be freely adjusted as users preference. 
Type of contact probe	Customizable with different size and shape probes

Sample Holder

Origin of the Hysteresis in I - V Curves for Planar Structure Perovskite Solar Cells Rationalized with a Surface Boundary-induced Capacitance Model

Ludmila Cojocaru,^{*1} Satoshi Uchida,^{*2} Piyankarage V. V. Jayaweera,³ Shoji Kaneko,³

Jotaro Nakazaki,¹ Takaya Kubo,¹ and Hiroshi Segawa^{*1}

¹Research Center for Advanced Science and Technology, The University of Tokyo, 4-6-1 Komaba, Meguro-ku, Tokyo 153-8904

²Komaba Organization for Educational Excellence College of Arts and Sciences, The University of Tokyo,

3-8-1 Komaba, Meguro-ku, Tokyo 153-8902

³SPD Laboratory, Inc., 2-35-1 Johoku, Naka-ku, Hamamatsu, Shizuoka 432-8011

(E-mail: cojocaru@dsc.rcast.u-tokyo.ac.jp, uchida@rcast.u-tokyo.ac.jp, csegawa@mail.ecc.u-tokyo.ac.jp)

For efficient hybrid solar cells based on organometal halide perovskites, the real origin of the I - V hysteresis became a big issue and has been discussed widely. In this study, simulated I - V curves of different equivalent circuit models were validated with experimental I - V curves of a planar perovskite solar cell with the power conversion efficiency (PCE) of 18.0% and 8.8% on reverse scan (from open circuit to short circuit) and forward scan (from short circuit to open circuit), respectively. We found that an equivalent circuit model with a series of double diodes, capacitors, shunt resistances, and single series resistance produces simulated I - V curves with large hysteresis matching with the experimentally observed curves. The electrical capacitances generated by defects due to the lattice mismatch at the $\text{TiO}_2/\text{CH}_3\text{NH}_3\text{PbI}_3$ and $\text{CH}_3\text{NH}_3\text{PbI}_3/\text{spiro-OMeTAD}$ interface are truly responsible for the hysteresis in perovskite solar cells.

Perovskite solar cells based on $\text{CH}_3\text{NH}_3\text{PbI}_3$ have attracted enormous attention in the last few years due to their outstanding performance as photovoltaics. The power conversion efficiency (PCE) of the devices has dramatically improved to over 20% in a relatively short duration.^{1,2} Despite the unique properties and higher efficiencies, several important issues, e.g., mysterious hysteresis in I - V curves and durability of stabilized performance, still remained for commercialization.^{3,4} It has been found the hysteresis strongly depends on the device architecture, where the planar structure and Al_2O_3 mesoporous perovskite cells show relatively large hysteresis than TiO_2 mesoporous structure devices.⁵ The typical planar structure of $\text{SnO}_2:\text{F}(\text{FTO})/\text{compact TiO}_2/\text{CH}_3\text{NH}_3\text{PbI}_3/\text{spiro-OMeTAD}/\text{Au}$ ⁶ suffers from severe hysteresis in the I - V measurement.^{3,4} The reverse scan (from the open circuit to the short circuit) always shows higher PCE than the forward scan (from short circuit to the open circuit). Hence, such hysteresis in the I - V curves creates ambiguity about the actual performance of the device, which is being suspected to be over-estimated.^{7,8}

The origin of hysteresis has been discussed on the intrinsic properties like ferroelectric polarization⁹ and/or ionic migration¹⁰ of the perovskite to date. However, there was no direct evidence that could support the above claims. It has been reported that passivation of TiO_2 layer by C60 or use of phenyl-C61-butyric acid methyl ester (PCBM) instead of TiO_2 in inverted device structure reduces the hysteresis.^{11–13} The passivation could minimize the trap states and improve electron transfer through the interface of $\text{TiO}_2/\text{CH}_3\text{NH}_3\text{PbI}_3$, resulting in the

reduction of hysteresis.¹¹ On the other hand, PCBM in the inverted cell could extract the carriers (electrons) more efficiently than TiO_2 without accumulation at the interface, and the hysteresis was eliminated. In another standpoint, lattice mismatch of the interfaces containing organic compounds could be ignored and consequently the hysteresis was reduced. The importance of lattice mismatch is widely known and discussed for inorganic thin film solar cells.¹⁴ Due to the higher expansion coefficient of $\text{CH}_3\text{NH}_3\text{PbI}_3$ than TiO_2 , an interfacial stress is created at the interface of $\text{TiO}_2/\text{CH}_3\text{NH}_3\text{PbI}_3$, which changes with temperature.^{15,16} The above reports strongly suggest that defects and/or traps at the interface between compact TiO_2 and $\text{CH}_3\text{NH}_3\text{PbI}_3$ play an important role in causing the hysteresis. The charge trapping/detrapping and/or charge accumulation caused by the lattice mismatch or voids at this interface act as capacitors. In the present study, we confirm “a double diode equivalent circuit model,” including the interfacial capacitive components, where the hysteresis essentially comes up due to carrier accumulation at the interfaces.

For the model study, we used high efficiency planar perovskite solar cells showing large hysteresis in the I - V curves. The planar structured perovskite solar cells using a TiO_2 substrate coated on flat FTO substrate (SPD laboratory, sheet resistance $7\ \Omega/\text{square}$, average transmittance in visible range 81%, and FTO thickness 800 nm) were fabricated by the one-step solution deposition method. $\text{CH}_3\text{NH}_3\text{PbI}_3$ was prepared using mixed halide precursors (PbCl_2 and $\text{CH}_3\text{NH}_3\text{I}$) dissolved in dimethylformamide (DMF), as described previously.^{17–19} Spiro-OMeTAD was used as a p-type hole extracting layer. Finally, a gold back contact layer was deposited on spiro-OMeTAD under vacuum by the thermal evaporation method. The cross-sectional SEM image of the device is shown in Figure 1. The device comprised a 50 nm compact TiO_2 layer, a 350 nm $\text{CH}_3\text{NH}_3\text{PbI}_3$, a 260 nm spiro-OMeTAD, and an 80 nm Au metal back contact (Figure 1). Photovoltaic characterization of the device was done by taking I - V curves under AM1.5G ($100\ \text{mW cm}^{-2}$) solar irradiation, measured by a reverse scan from +1.2 to $-0.05\ \text{V}$ and forward scan (from -0.05 to +1.2 V), active area $0.0314\ \text{cm}^2$. I - V curves (Figure 2) of the cell showed large hysteresis. Table 1 lists the photovoltaic parameters of the cell; reverse scan PCE of 18.0%, $J_{\text{sc}} = 24.0\ \text{mA cm}^{-2}$, $V_{\text{oc}} = 1.034\ \text{V}$, and FF = 0.73, forward scan PCE of 8.8%, $J_{\text{sc}} = 23.9\ \text{mA cm}^{-2}$, $V_{\text{oc}} = 0.852\ \text{V}$, and FF = 0.43.

In order to validate hysteresis in I - V characteristics, we considered several equivalent circuit models and obtained I - V

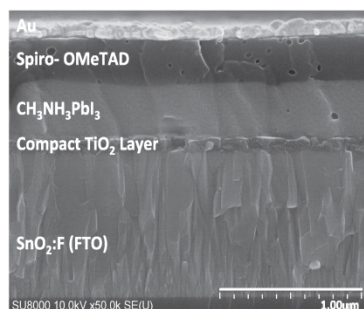


Figure 1. Cross-sectional SEM image of perovskite solar cells deposited on flat FTO substrate.

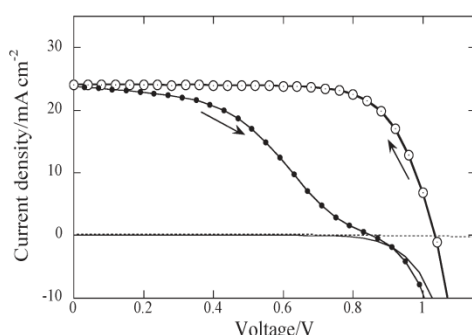


Figure 2. I - V curves for photovoltaic device based on planar structure perovskite solar cells measured at different scan directions (black dots forward scan, circle for reverse scan) under AM1.5G (100 mW cm^{-2}).

Table 1. Photovoltaic parameters extracted from I - V curves for the best planar structure perovskite solar cell

Scan directions	$J_{sc}/\text{mA cm}^{-2}$	V_{oc}/V	FF	PCE/%
Reverse	24.0	1.034	0.73	18.0
Forward	23.9	0.852	0.43	8.8

curves by simulation using MultiSim Electronic Workbench application (from National Instruments). The widely used equivalent circuit of a solar cell comprises a diode, a series resistance (R_s), and shunt resistance (R_{sh}) (Figure S1). The series resistance (R_s) represents the total resistance of the device, while the shunt resistance (R_{sh}) represents the resistance to leakage current. The above standard equivalent circuit was built on the Multisim's onscreen circuit board. In this simulation, we used a modulation power source as shown V1 in the Figure S1, Figure S2, and Figure 3. Voltage V2 shown in Figure S1 controls the frequency of triangle wave, which represents the scan speed of I - V curves. The voltage was linearly swept with the triangle wave as shown in Figure S3 to simulate the reverse scan and forward scan. To plot I - V curves across the simulated cell was monitored onscreen oscilloscope provided in the software. Two input channels are assigned: A for the measured voltage at both ends of dummy resistance R_3 to evaluate the current and B for voltage.

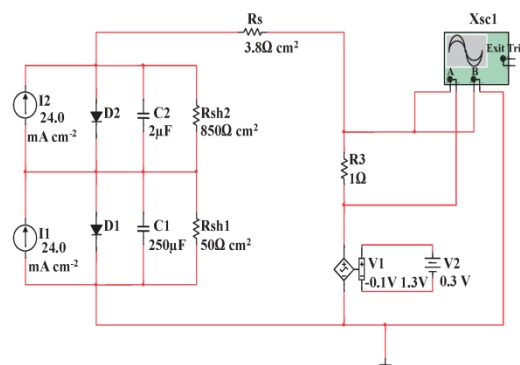


Figure 3. Equivalent circuit model of perovskite solar cell with double diodes, capacitances, R_{sh} and single R_s .

Initially, R_s and R_{sh} values were set to calculate series and shunt resistance of the experimental I - V curve for reverse scan. Experimental I - V curve was successfully simulated with $R_s = 3.8 \Omega \text{ cm}^2$ and $R_{sh} = 900 \Omega \text{ cm}^2$ by confirming accuracy of the model simulation method. As shown in Figure S1, the simulated I - V curves did not change with the scan directions. This confirmed that the standard equivalent circuit having a single diode with a series and a shunt resistance does not hold good I - V simulation showing hysteresis. Then, taking the carrier accumulation into account, we incorporated a capacitor in parallel to R_{sh} in the equivalent circuit (Figure S2). However, adding a capacitor to the standard equivalent circuit also did not simulate the experimental hysteric I - V curves (Figure S2). Finally, we tested an equivalent circuit model (Figure 3) composed of two diodes connected in series, two capacitors, two shunt resistances (R_{sh}), single series resistance (R_s), and two current sources.

The fitting parameters of the circuit model for the simulated I - V curves are summarized in Table S1. For this model, fitting parameters (R_s , R_{sh1} , and R_{sh2}) were chosen by using calculated series and shunt resistance values from the experimental I - V data (Figure 2). The initial $C1$ and $C2$ were randomly selected. Then, parameters were optimized (by trial and error method) to minimize deviation between the simulated and experimental curves.

As shown in Figure 4, the simulated I - V curves of this double diode equivalent circuit showed hysteresis, matching closely with the experimental I - V curves. According to this equivalent circuit model, perovskite solar cells may consist of two active junctions with drastically different capacitances developed from carrier accumulation at the interfaces. The $\text{CH}_3\text{NH}_3\text{PbI}_3$ layer is sandwiched between n- and p-type contacts and formed two interfaces. It has been already reported that $\text{CH}_3\text{NH}_3\text{PbI}_3$ forms two active junctions: one with the n-type TiO_2 and the other with p-type spiro-OMeTAD.²⁰ The interface between TiO_2 and $\text{CH}_3\text{NH}_3\text{PbI}_3$ shows a huge lattice mismatch.¹⁵ These mismatches produce high electrical capacitance at the interface. On the other hand, the interface between the spiro-OMeTAD/ $\text{CH}_3\text{NH}_3\text{PbI}_3$ layer having less mismatch creates a relatively smaller capacitive component at the interface. Hence, in the equivalent circuit model, we attribute the first part comprising a diode ($D2$), large capacitor ($C2$), and shunt

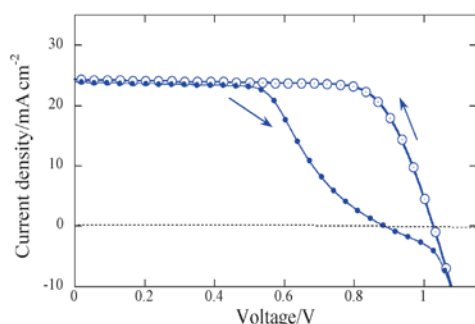


Figure 4. Simulated I - V curves with hysteresis using double diodes, capacitors, R_{sh} and single R_s model for perovskite solar cell. The extracted photovoltaic characteristics are shown in Figure S1.

resistance (R_{sh2}) to the $\text{TiO}_2/\text{CH}_3\text{NH}_3\text{PbI}_3$ interface. The second part with a diode ($D1$), single smaller capacitance ($C1$), and shunt resistance (R_{sh1}) can be attributed to the $\text{CH}_3\text{NH}_3\text{PbI}_3/\text{spiro-OMeTAD}$ interface.

In conclusion, we clarified the origin of hysteresis in the I - V curves of a planar perovskite cell using different equivalent circuit models and simulation of their I - V curves. A planar cell showing huge hysteresis, PCE of 18.0% on reverse, and 8.8% on forward scan was used for validating the equivalent circuits. We found that the standard equivalent circuit with a diode, series resistance, and shunt resistance does not reproduce the hysteresis of I - V curves. Even for the incorporation of a capacitive component in the circuit, the model also did not match the experimental I - V curves. However, an equivalent circuit model composed of two series connected diodes, two capacitors, two shunt resistances, and a series resistance reproduced the hysteresis of the experimental I - V curves. This result suggests that the perovskite cell has two active interfaces: $\text{TiO}_2/\text{CH}_3\text{NH}_3\text{PbI}_3$ and $\text{CH}_3\text{NH}_3\text{PbI}_3/\text{spiro-OMeTAD}$. The hysteresis is essentially caused by carrier accumulation at these active interfaces. We believe that the lattice mismatch or voids present at the $\text{TiO}_2/\text{CH}_3\text{NH}_3\text{PbI}_3$ interface create high electrical capacitance and the other interface with less defects exhibits low capacitance, where hysteresis was in good agreement with the simulation.

The authors thanks for financial supports from New Energy and Industrial Technology Development Organization (NEDO, Japan).

Supporting Information is available electronically on J-STAGE.

References and Notes

- 1 M. A. Green, K. Emery, Y. Hishikawa, W. Warta, E. D. Dunlop, *Prog. Photovolt. Res. Appl.* **2015**, *23*, 1.
- 2 T. Miyasaka, *Chem. Lett.* **2015**, *44*, 720.
- 3 A. K. Jena, H.-W. Chen, A. Kogo, Y. Sanehira, M. Ikegami, T. Miyasaka, *ACS Appl. Mater. Interfaces* **2015**, *7*, 9817.
- 4 H.-S. Kim, N.-G. Park, *J. Phys. Chem. Lett.* **2014**, *5*, 2927.
- 5 H. J. Snaith, A. Abate, J. M. Ball, G. E. Eperon, T. Leijtens, N. K. Noel, S. D. Stranks, J. T.-W. Wang, K. Wojciechowski, W. Zhang, *J. Phys. Chem. Lett.* **2014**, *5*, 1511.
- 6 M. Liu, M. B. Johnston, H. J. Snaith, *Nature* **2013**, *501*, 395.
- 7 Editorial: *Nat. Photonics* **2014**, *8*, 665.
- 8 Editorial: *Nat. Mater.* **2014**, *13*, 837.
- 9 J. Wei, Y. Zhao, H. Li, G. Li, J. Pan, D. Xu, Q. Zhao, D. Yu, *J. Phys. Chem. Lett.* **2014**, *5*, 3937.
- 10 W. Tress, N. Marinova, T. Moehl, S. M. Zakeeruddin, M. K. Nazeeruddin, M. Grätzel, *Energy Environ. Sci.* **2015**, *8*, 995.
- 11 K. Wojciechowski, S. D. Stranks, A. Abate, G. Sadoughi, A. Sadhanala, N. Kopidakis, G. Rumbles, C.-Z. Li, R. H. Friend, A. K.-Y. Jen, H. J. Snaith, *ACS Nano* **2014**, *8*, 12701.
- 12 M. Shahiduzzaman, K. Yamamoto, Y. Furumoto, T. Kuwabara, K. Takahashi, T. Taima, *Chem. Lett.* **2015**, in press. doi:10.1246/cl.150814.
- 13 C.-G. Wu, C.-H. Chiang, Z.-L. Tseng, Md. K. Nazeeruddin, A. Hagfeldt, M. Grätzel, *Energy Environ. Sci.* **2015**, *8*, 2725.
- 14 G.-C. Park, H.-D. Chung, C.-D. Kim, H.-R. Park, W.-J. Jeong, J.-U. Kim, H.-B. Gu, K.-S. Lee, *Sol. Energy Mater. Sol. Cells* **1997**, *49*, 365.
- 15 L. Cojocaru, S. Uchida, Y. Sanehira, V. Gonzalez-Pedro, J. Bisquert, J. Nakazaki, T. Kubo, H. Segawa, *Chem. Lett.* **2015**, *44*, 1557.
- 16 T. J. Jacobsson, L. J. Schwan, M. Ottosson, A. Hagfeldt, T. Edvinsson, *Inorg. Chem.* **2015**, Article ASAP. doi:10.1021/acs.inorgchem.5b01481.
- 17 L. Cojocaru, S. Uchida, Y. Sanehira, J. Nakazaki, T. Kubo, H. Segawa, *Chem. Lett.* **2015**, *44*, 674.
- 18 L. Cojocaru, S. Uchida, A. K. Jena, T. Miyasaka, J. Nakazaki, T. Kubo, H. Segawa, *Chem. Lett.* **2015**, *44*, 1089.
- 19 A. Kogo, Y. Numata, M. Ikegami, T. Miyasaka, *Chem. Lett.* **2015**, *44*, 829.
- 20 E. Edri, S. Kirmayer, S. Mukhopadhyay, K. Gartsman, G. Hodes, D. Cahen, *Nat. Commun.* **2014**, *5*, 3461.

SCIENTIFIC REPORTS

OPEN

Determination of unique power conversion efficiency of solar cell showing hysteresis in the I-V curve under various light intensities

Received: 17 February 2017

Accepted: 17 August 2017

Published online: 18 September 2017

Ludmila Cojocar¹, Satoshi Uchida², Koichi Tamaki³, Piyankarage V. V. Jayaweera³, Shoji Kaneko³, Jotaro Nakazaki⁴, Takaya Kubo¹ & Hiroshi Segawa^{1,4}

Energy harvesting at low light intensities has recently attracted a great deal of attention of perovskite solar cells (PSCs) which are regarded as promising candidate for indoor application. Anomalous hysteresis of the PSCs a complex issue for reliable evaluation of the cell performance. In order to address these challenges, we constructed two new evaluation methods to determinate the power conversion efficiencies (PCEs) of PSCs. The first setup is a solar simulator based on light emitting diodes (LEDs) allowing evaluation of the solar cells at wider range of light intensities, ranging from 10^2 to 10^{-3} $\text{mW}\cdot\text{cm}^{-2}$. As the overestimate error, we found that the PCEs of dye sensitized solar cell (DSC) and PSCs increase dramatically at low light intensities conditions. Due to the internal capacitance at the interfaces on hybrid solar cells, the measurement of current below 10^{-2} $\text{mW}\cdot\text{cm}^{-2}$ shows constant value given high PCE, which is related to the capacitive current and origin of the hysteresis. The second setup is a photovoltaic power analyzing system, designed for tracking the maximum power (P_{max}) with time. The paper suggests the combination of the LED solar simulator and P_{max} tracking technique as a standard to evaluate the PCE of capacitive solar cells.

Efficient power generation under weak irradiation is essential for indoor applications or installation and installation in cloudy places. However, solar cells performances is usually evaluated by solar simulators with 10^3 $\text{mW}\cdot\text{cm}^{-2}$ irradiance (AM1.5 G) as described in IEC 60904-3 etc., as seen in the solar cell efficiency tables¹. This condition (1 sun) is almost equivalent to direct sunlight at AM1.5 G. In the case of dye-sensitized solar cells (DSCs) and perovskite solar cells (PSCs), better performances have been reported under weak irradiation conditions²⁻⁶. Performance measurement of solar cells at very low irradiance levels is not well established yet, their measurement conditions depended largely on the measurement parameters. Establishing a standardized method for evaluation under weak irradiation is a necessary step for reliable reports on PCE of solar cells designed for indoor application.

The general method to determine the PCE of solar cells is to measure the photocurrent by scanning the bias potential. The results are expressed as a current density – voltage (J - V) curve or an output electric power – voltage (P - V) curve, and the ratio of the maximum output power (P_{max}) to the irradiation intensity is described as the conversion efficiency (η). Therefore, accurate current – voltage (J - V) measurement is essential for the evaluation of solar cells. However, the anomalous I - V hysteresis of PSCs⁷⁻⁹ is a problem for reliable evaluation of the PCE. Since different I - V curves are obtained depending on the voltage scan direction, two efficiency values are obtained for a device. The recent rapid rise of PSCs, which exhibit PCEs more than 22%¹⁰, demands accurate determination of the PCE values. There are reports on evaluation the PCE by continuous measurement of photocurrent under applied bias potential, where P_{max} was obtained^{11,12}. However, the temporal change in P_{max} could not be followed.

¹Research Center for Advanced Science and Technology, The University of Tokyo, Komaba 4-6-1, Meguro-ku, Tokyo, 153-8904, Japan. ²Komaba Organization for Educational Excellence, Faculty of Arts and Sciences, The University of Tokyo, Komaba 3-8-1, Meguro-ku, Tokyo, 153-8902, Japan. ³SPD Laboratory, Inc., Johoku 2-35-1, Naka-ku, Hamamatsu, 432-8011, Japan. ⁴Department of General Systems Studies, Graduate School of Arts and Sciences, The University of Tokyo, Komaba 3-8-1, Meguro-ku, Tokyo, 153-8902, Japan. Correspondence and requests for materials should be addressed to L.C. (email: cojocar@dstc.rcast.u-tokyo.ac.jp) or S.U. (email: uchida@rcast.u-tokyo.ac.jp) or H.S. (email: csegawa@mail.ecc.u-tokyo.ac.jp)



SPD Laboratory, Inc.

2-35-1 Johoku, Hamamatsu,
432-8011,
JAPAN

Tel: +81-53-474-7901

Fax: +81-53-401-7080

Email: inq@spd-lab.com

Web: <http://www.spdlab.com/English/Home.html>

September 2022